



UNIVERSIDADE ESTADUAL DE CAMPINAS
Faculdade de Engenharia Mecânica
Instituto de Geociências

CRISTIAN RICARDO MENDOZA BLANCO

**Characterization and Modeling of Fractures
Using Borehole Image Logs and Seismic
Attributes for The Pre-Salt Section of The
Santos Basin, Brazil**

**Caracterização e Modelagem de Fraturas
Usando Perfis de Imagem de Poços e
Atributos Sísmicos para o Pré-Sal da Bacia de
Santos, Brasil**

CAMPINAS

2022

CRISTIAN RICARDO MENDOZA BLANCO

Characterization and Modeling of Fractures Using Borehole Image Logs and Seismic Attributes for The Pre-Salt Section of The Santos Basin, Brazil

Caracterização e Modelagem de Fraturas Usando Perfis de Imagem de Poços e Atributos Sísmicos para o Pré-Sal da Bacia de Santos, Brasil

Dissertation presented to the School of Mechanical Engineering and Institute of Geosciences of the University of Campinas in partial fulfillment of the requirements for the degree of Master in Science and Petroleum Engineering in the area of reservoirs and management.

Dissertação apresentada à Faculdade de Engenharia Mecânica e Instituto de Geociências da Universidade Estadual de Campinas como parte dos requisitos exigidos para a obtenção do título de Mestre em Ciências e Engenharia de Petróleo, na Área de reservatórios e gestão.

Orientador: Prof. Dr. Alexandre Campanhe Vidal

ESTE TRABALHO CORRESPONDE À VERSÃO
FINAL DA DISSERTAÇÃO DEFENDIDA PELO
ALUNO CRISTIAN RICARDO MENDOZA BLANCO
E ORIENTADA PELO PROF. DR. ALEXANDRE
CAMPANE VIDAL.

CAMPINAS

2022

Ficha catalográfica
Universidade Estadual de Campinas
Biblioteca da Área de Engenharia e Arquitetura
Rose Meire da Silva - CRB 8/5974

M523c Mendoza Blanco, Cristian Ricardo, 1987-
Characterization and modeling of fractures using borehole image logs and seismic attributes for the pre-salt section of the Santos basin, Brazil / Cristian Ricardo Mendoza Blanco. – Campinas, SP : [s.n.], 2022.

Orientador: Alexandre Campanhe Vidal.
Dissertação (mestrado) – Universidade Estadual de Campinas, Faculdade de Engenharia Mecânica.

1. Fraturas (Geologia). 2. Pré-sal - Brasil. 3. Falhas (Geologia). 4. Ondas sísmicas. 5. prospecção sísmica. I. Vidal, Alexandre Campanhe, 1969-. II. Universidade Estadual de Campinas. Faculdade de Engenharia Mecânica. III. Título.

Informações Complementares

Título em outro idioma: Caracterização e modelagem de fraturas usando perfis de imagem de poços e atributos sísmicos para o pré-sal da bacia de Santos, Brasil

Palavras-chave em inglês:

Fractures (Geology)

Pre-salt - Brazil

Faults (Geology)

Seismic waves

Seismic prospection

Área de concentração: Reservatórios e Gestão

Titulação: Mestre em Ciências e Engenharia de Petróleo

Banca examinadora:

Alexandre Campanhe Vidal [Orientador]

Michelle Chaves Kuroda

Aline Maria Pocas Belila

Data de defesa: 01-08-2022

Programa de Pós-Graduação: Ciências e Engenharia de Petróleo

Identificação e informações acadêmicas do(a) aluno(a)

- ORCID do autor: <https://orcid.org/0000-0003-4380-2882>

- Currículo Lattes do autor: <https://lattes.cnpq.br/3757416969640676>

**UNIVERSIDADE ESTADUAL DE CAMPINAS
FACULDADE DE ENGENHARIA MECÂNICA
E INSTITUTO DE GEOCIÊNCIAS**

DISSERTAÇÃO DE MESTRADO ACADÊMICO

**Characterization and Modeling of Fractures
Using Borehole Image Logs and Seismic
Attributes for The Pre-Salt Section of The
Santos Basin, Brazil**

**Caracterização e Modelagem de Fraturas
Usando Perfis de Imagem de Poços e
Atributos Sísmicos para o Pré-Sal da Bacia de
Santos, Brasil**

Autor: Cristian Ricardo Mendoza Blanco

Orientador: Prof. Dr. Alexandre Campana Vidal

A Banca Examinadora composta pelos membros abaixo aprovou esta Dissertação:

**Prof. Dr. Alexandre Campana Vidal, Presidente
DGRE/IGE/UNICAMP**

**Dra. Michelle Chaves Kuroda
Centro de Estudos de Petróleo, CEPETRO/UNICAMP**

**Dra. Aline Maria Poças Belila
Equinor, Brasil**

A Ata de Defesa com as respectivas assinaturas dos membros encontra-se no SIGA/Sistema de Fluxo de Dissertação/Tese e na Secretaria do Programa da Unidade.

Campinas, 01 de agosto de 2022

Dedicatória

A Deus por me dar saúde, força e sabedoria para realizar meus sonhos.

À minha família pelo grande apoio.

A Dios por brindarme salud, fortaleza y sabiduría para cumplir mis sueños.

A mi familia por su gran apoyo.

Agradecimento

Agradeço primeiramente a Deus por me dar a oportunidade de concluir meu mestrado, por me dar saúde, sabedoria e força para cumprir esse objetivo traçado em minha vida.

Agradeço aos meus pais Pedro Mendoza e Fanny Blanco, meu filho Sebastian Mendoza, minha esposa Yina Urquijo, meus irmãos Laura e Darwin e minha avó Teresa Figueroa, por serem meu grande apoio mesmo a distância e por sempre me aconselharem para que eu obtivesse sucesso nos meus objetivos.

Um agradecimento especial ao meu orientador Professor Doutor Alexandre Campana Vidal pela oportunidade que me foi dada, pela confiança, apoio, ensino e pelas excelentes sugestões para meu crescimento profissional.

Ao Laboratório de Modelagem Geológica de Reservatórios e seu grupo de profissionais pelo grande apoio no desenvolvimento do meu projeto, em especial aos meus parceiros Guilherme Chinelatto, Mateus Basso, Jean Rangel, Juan Villacreses e Oton Rubio pelas sugestões, conselhos e suporte.

Aos membros da banca Dr. Bruno César Zanardo Honório e Dra. Michelle Chaves Kuroda por aceitarem fazer parte da qualificação deste projeto e pelas contribuições e sugestões feitas para a melhoria do meu trabalho. Também à Dra. Aline Belila por aceitarem fazer parte da banca da defesa contribuindo com seus conhecimentos visando alcançar excelentes resultados e meu crescimento profissional.

Agradeço a empresa Equinor pela oportunidade de trabalhar em associação com o seu projeto.

O presente trabalho foi realizado com apoio da Fundação de Amparo à Pesquisa do Estado de São Paulo (FAPESP), processo no 2020/02130-2.

À Universidade Estadual de Campinas e seu excelente grupo de professores.

Resumo

A Bacia offshore de Santos é uma bacia prolífica com grande potencial para exploração de hidrocarbonetos, em parte devido à sua evolução tectônica e estratigrafia associada a carbonatos lacustres descobertos nas águas profundas brasileiras embaixo do sal. A alta permeabilidade nesta bacia é provavelmente controlada por altas intensidades de fratura e dissolução de carbonato, portanto, prever o comportamento de fraturas naturais nesses depósitos ajudará a entender seus efeitos no fluxo de fluido e na produtividade do reservatório. Este estudo se concentra na construção de um modelo de rede de fratura discreta com base na compreensão da intensidade, orientação e distribuição espacial das fraturas, isso foi realizado por meio do uso de ferramentas como registros de imagem de poço de 4 poços e sísmica 3-D. A partir dessas ferramentas foi possível identificar os principais horizontes (topo e base do play do pré-sal), falhas regionais, interpretação das fraturas e do estado de tensão in situ no play do pré-sal da Bacia de Santos. Neste trabalho, descobrimos que, de acordo com os breakouts e as fraturas induzidas por perfuração, a tensão horizontal máxima (SHmax) tem um azimute NE-SW, que comparado com a orientação e regime de estruturas de grande escala sísmica no reservatório, é possível destacar que a área de estudo é influenciada por um padrão normal de falha e configuração de tensão extensional. Além disso, de acordo com as fraturas naturais, identificamos quatro sets, os sets 1 e 2 seguem uma direção paralela a SHmax NE-SW e os sets 3 e 4 seguem uma direção paralela a Shmin. Em relação à caracterização das redes de fraturas, distribuímos os atributos de fratura no grid geológica de acordo com parâmetros como densidade de fraturas, abertura de fratura, comprimento de fratura e orientação de fratura, esses parâmetros permitiram quantificar a porosidade e permeabilidade da fratura, destacando assim regiões com as melhores respostas de permeabilidade de fratura.

Palavras-chave: Bacia de Santos, Seção pre-sal, Redes de Fratura, Atributos Sísmicos, Interpretação Sísmica.

Abstract

The offshore Santos Basin is a prolific basin with great potential for exploration of hydrocarbons, this due in part to its tectonic evolution and stratigraphy associated with lacustrine carbonates discovered in the Brazilian deep-water underneath the salt. The high permeability in this basin is likely controlled by high fracture intensities and carbonate dissolution, therefore, predicting the behavior of natural fractures in these deposits will help to understand their effects on fluid flow and reservoir productivity. This study focuses on the construction of a discrete fracture network model based on the understanding of intensity, orientation, and spatial distribution of the fractures, this was accomplished through the use of tools such as borehole image logs of 4 wells, and 3-D seismic data. From these tools was possible to identify the main horizons (top and base of the pre-salt play), regional faults, as well as allowed the interpretation of fractures and the in-situ stress state in the pre-salt play of the Santos Basin. In this work, we found that in accordance with the borehole breakouts and drilling-induced fractures the maximum horizontal stress (SH_{max}) has an azimuth NE-SW, which compared with the orientation and regime of large seismic scale structures in the reservoir, it is possible to highlight that the study area is influenced by a normal fault pattern and extensional stress configuration. In addition, according to open natural fractures we identified four sets, of which set 1 and 2 follow a strike parallel to SH_{max} NE-SW and sets 3 and 4 follow a strike parallel to Sh_{min} . Regarding the characterization of the fracture networks, we distributed the fracture attributes in the geological grid according to parameters such as density of fractures, fracture aperture, fracture length, and fracture orientation, these parameters allowed to quantify the fracture porosity and permeability, thus highlighting regions with the best fracture permeability responses.

Keywords: Santos Basin, Pre-salt Section, Fracture networks, Seismic attributes, Seismic interpretation.

List of Figures

Article 1: FRACTURE CHARACTERIZATION AND IN-SITU STRESS DETERMINATION USING BOREHOLE IMAGE LOGS AND SEISMIC DATA: THE PRE-SALT SECTION OF THE SANTOS BASIN, BRAZIL

Figure 1. Location map of the study area and the Brazilian pre-salt section, situated in the SE offshore continental margin of the Santos basins. (Shapefiles taken from the Brazilian National Agency for Petroleum, Natural Gas and Biofuels, ANP).

Figure 2. Lithostratigraphic chart of the rift and post-rift super-sequences of the Santos Basin. (Extracted from Moreira et al., 2007).

Figure 3. Workflow used to highlight faults and discontinuities from seismic attributes. Results illustrate the interpreted horizons and intersections with faults.

Figure 4. Seismic cross-section showing the noise-reduction filter. (A) Original seismic. (B) After dip steered median filter (DSMF).

Figure 5. Seismic attributes executed to highlight discontinuities. (A) Variance. (B) Ant tracking. (C) Ant tracking overlaid with original seismic.

Figure 6. Visualization of natural fractures, drilling induced fractures and breakouts in acoustic borehole images. A) Occurrences of open and enlarged natural fracture pointed by the white arrow and B) Irregular and vertical drilling induced fractures pointed by the blue arrow and breakouts highlighted in green area. Note that natural fractures have lateral continuity while DIF are irregular and vertically arranged, furthermore the DIF are arranged 90° of the orientation of breakouts.

Figure 7. A) In-situ stress state is defined by: vertical stress (S_v), maximum principal horizontal stress (S_{Hmax}) and minimum principal horizontal stress (S_{Hmin}) (Extracted from Huapeng Niu et al., 2019). B) Typical borehole breakout and drilling-induced fractures. The S_{Hmax} is

approximately perpendicular to the breakouts, and parallel to drilling-induced fractures (Extracted from H. Talebi et al., 2018).

Figure 8. Workflow used to fracture characterization from borehole image logs.

Figure 9. A) 2D map of the Barra Velha Formation top surface. Showing the seismic cross section (A-A') on the yellow line. B) Seismic cross section (A-A') before interpretation. C) Interpreted seismic section (A-A') of the main horizons (top and base of the pre-salt play, green and yellow lines respectively) and regional faults (black lines) of the study area. D) Zooming in on the intersection of the sonic log (Well D) with the seismic, showing the strong change between the interpreted horizons, the salt and the basement.

Figure 10. A) 2D map of the Camboriu Formation top surface. Showing the seismic cross section (B-B') on the yellow line. B) Seismic cross section (B-B') before interpretation. C) Interpreted seismic section (B-B') of the main horizons (top and base of the pre-salt play, green and yellow lines respectively) and regional faults (black lines) of the study area. D) Zooming in on the intersection of the sonic log (Well A) with the seismic, showing the strong change between the interpreted horizons, the salt and the basement.

Figure 11. Regional structural framework of the pre-salt play in the study area characterized by high-angle normal faulting.

Figure 12. The orientation of the minimum horizontal stress (S_{hmin}) and the maximum horizontal stress (S_{Hmax}) determined from the borehole breakout and drilling-induced fractures.

Figure 13. Maximum and minimum horizontal stress analysis. A) Demonstration of the structural configuration of the study area based on breakouts and drilling-induced fractures. B) Model that the study area is influenced by a normal stress configuration, defined by the relation $S_v > S_{Hmax} > S_{hmin}$, according to normal fault stress regime (Anderson, 1905).

Figure 14. Fractures expressions and fracture intensity log of well A and Well B.

Figure 15. Fractures expressions and fracture intensity log of well C and Well D.

Figure 16. A) Fault and large fracture patches extracted by ant tracking algorithm, B) illustrating the prominent strike direction NE-SW on stereo net diagram. C) illustrating dip directions NW and SE.

Figure 17. Evaluation of open and closed natural fractures. A) Illustrating four sets in the pre-salt play. stereo net diagram representing the Dip azimuth. B) Stereo net diagram highlighting the two main sets with a strike NE-SW parallel to SHmax. C) Stereo net diagram highlighting the two sets with a lower prevalence with a strike NW-SE orthogonal to SHmax.

Figure 18. Summary plot of the main fracture sets identified in the pre-salt play from borehole image logs.

Article 2: DISCRETE FRACTURE NETWORK MODELING BASED ON FRACTURE INTENSITY DERIVED FROM BOREHOLE IMAGE LOGS AND SEISMIC ATTRIBUTES BY INCORPORATING SUPERVISED NEURAL NETWORKS: THE PRE-SALT SECTION OF THE SANTOS BASIN, BRAZIL

Figure 19. Location map of the study area and the Brazilian pre-salt section, situated in the SE offshore continental margin of the Santos basins. (Shapefiles taken from the Brazilian National Agency for Petroleum, Natural Gas and Biofuels, ANP).

Figure 20. Lithostratigraphic chart of the rift and post-rift super-sequences of the Santos Basin. (Extracted from Moreira et al., 2007).

Figure 21. Acoustic image logs. A) Occurrences of natural fracture. B) Breakouts highlighted in green area. C) Representative breakout and drilling-induced fractures. The SHmax is approximately perpendicular to the breakouts, and parallel to drilling-induced fractures.

Figure 22. Schematic example: zones without information to obtain a good distribution of the fracture intensity. The fracture intensity is limited to the wellbore and its distribution is highly uncertain for the regions away from the well.

Figure 23. Global system of neural network processing used in this study.

Figure 24. Summary plot of the main fracture sets identified in the pre-salt play from borehole image logs. A) The borehole breakout and drilling-induced fractures determined the orientation of the minimum horizontal stress (S_{hmin}) and maximum horizontal stress (S_{Hmax}). B) Four fracture sets in pre-salt play are illustrated. The Dip azimuth is represented by a stereo net diagram. C) Illustrating the two main sets with a strike NE-SW parallel to S_{Hmax} . D) Illustrating the two sets with a lower prevalence with a strike NW-SE orthogonal to S_{Hmax} . E) Representative plot of the fracture sets identified in the pre-salt play from borehole image logs.

Figure 25. A) Seismic cross section (A-A') before interpretation. B) Interpreted seismic section (A-A') of the main horizons (top and base of the pre-salt play, green and yellow lines respectively) and regional faults (black lines).

Figure 26. 3D geological grid highlighting its dimensions for upscaling fracture properties.

Figure 27. The upscaled fracture Intensity property is populated throughout the 3D grid.

Figure 28. Permeability distribution (unscaled) obtained for each test varying the apertures of the fractures (0,5 mm, 0,4 mm and 0,3 mm).

Figure 29. A) Results of the correlation analysis between the seismic attributes selected as input data for training in the supervised technique. B) Seismic attributes selected considering that are algorithms dedicated to highlight fault and large fractures zones.

Figure 30. Stochastic DFN model built using the Fracture Intensity derived from the supervised neural network and the orientation interval for four fracture sets.

Figure 31. DFN fracture models for each fracture sets: Set 1 and 2 follow a strike NE-SW with average dip of 45° and 37° respectively; Set 3 and 4 follow a strike NW-SE with average dip of 53° and 43° respectively.

Figure 32. Fracture permeability (I, J, and K directions) for the grid DFN.

Figure 33. 2D view showing the grid direction (K_i and K_j) and the demonstration of the structural configuration of the study area.

Figure 34. Three fracture zones (red circles) belonging to Sets 1 and 2, highlighting the large number of fractures in the " K_j " direction and corresponding to the structural highs, suggesting areas with possible good permeability and fracture connectivity.

APPENDIX

Figure 35. Interpreted natural fractures, breakouts and drilling induced fractures at well A. A) Static image log. B) Dynamic Image log. C) Dip angle of natural fractures in tadpole. D) Rose diagram of the natural fractures showing strike azimuth. E) Dip angle of breakouts and drilling induced fractures in tadpole. F) Rose diagram of breakouts and drilling induced fractures showing strike.

Figure 36. Interpreted natural fractures, breakouts and drilling induced fractures at well B. A) Static image log. B) Dynamic Image log. C) Dip angle of natural fractures in tadpole. D) Rose diagram of the natural fractures showing strike azimuth. E) Dip angle of breakouts and drilling induced fractures in tadpole. F) Rose diagram of breakouts and drilling induced fractures showing strike.

Figure 37. Interpreted natural fractures, breakouts and drilling induced fractures at well C. A) Static image log. B) Dynamic Image log. C) Dip angle of natural fractures in tadpole. D) Rose diagram of the natural fractures showing strike azimuth. E) Dip angle of breakouts and drilling induced fractures in tadpole. F) Rose diagram of breakouts and drilling induced fractures showing strike.

Figure 38. Interpreted natural fractures, breakouts and drilling induced fractures at well D. A) Static image log. B) Dynamic Image log. C) Dip angle of natural fractures in tadpole. D) Rose diagram of the natural fractures showing strike azimuth. E) Dip angle of breakouts and drilling induced fractures in tadpole. F) Rose diagram of breakouts and drilling induced fractures showing strike.

Figure 39. Ant-Tracking Workflow.

Figure 40. Comparison amplitude spectra. A) Original seismic. B) Dip-Steered Median Filter (DSMF).

Table of Contents

INTRODUCTION	17
ARTICLE 1: FRACTURE CHARACTERIZATION AND IN-SITU STRESS DETERMINATION USING BOREHOLE IMAGE LOGS AND SEISMIC DATA: THE PRE-SALT SECTION OF THE SANTOS BASIN, BRAZIL.....	19
ABSTRACT	19
INTRODUCTION.....	19
GEOLOGICAL SETTING.....	20
DATABASE	23
METHODS	23
Horizons and Faults Interpretation.....	23
Borehole Image Logs.....	26
RESULTS AND DISCUSSION.....	29
Seismic Interpretation (Horizons and Faults)	29
Interpretation and analysis of breakouts and drilling-induced fractures (In-situ stress analysis)	32
Interpretation and analysis of well fractures data	34
CONCLUSIONS.....	39
REFERENCES.....	39
ARTICLE 2: DISCRETE FRACTURE NETWORK MODELING BASED ON FRACTURE INTENSITY DERIVED FROM BOREHOLE IMAGE LOGS AND SEISMIC ATTRIBUTES BY INCORPORATING SUPERVISED NEURAL NETWORKS: THE PRE-SALT SECTION OF THE SANTOS BASIN, BRAZIL	49
ABSTRACT	49

INTRODUCTION.....	50
GEOLOGICAL SETTING.....	51
DATABASE AND METHODS	53
Interpretation of fractures in image logs.....	53
Fracture Modeling (Discrete Fracture Network – DFN)	54
Supervised Artificial Neural Networks for DFN	55
Model Upscaling.....	57
RESULTS AND DISCUSSION.....	57
Fracture Modeling (Discrete Fracture Network – DFN)	57
Supervised Artificial Neural Networks for DFN	60
Model Upscaling	63
CONCLUSIONS.....	66
REFERENCES.....	67
CONCLUSIONS.....	75
APPENDIX 1 - INTERPRETATION OF NATURAL FRACTURES, BREAKOUTS AND DRILLING INDUCED FRACTURES.....	76
APPENDIX 2 – ANT TRACKING WORKFLOW.....	79
APPENDIX 3 – SEISMIC DATA CONDITIONING	80
REFERENCES	81

INTRODUCTION

The recent discoveries of vast hydrocarbon accumulations in lacustrine carbonates from Brazil, Africa, and China have increased the scientific interest for a better understanding of the formation and evolution of these reservoirs (Herlinger et al., 2017). Moreover, the discovery of large oil accumulations in the Brazilian deep-water offshore basins underneath the salt, which contains lacustrine carbonates have opened a new exploratory frontier. The occurrence of this new play has brought significant economic prosperity for Brazil, translated into reducing its energy dependence and making the country one of the world's largest producers of oil and gas (Riccomini et al., 2012).

The Brazilian pre-salt section is located in the SE offshore continental margin of the Campos and Santos Basins, and is a prominent oil-bearing sequence of carbonate rocks, overlaid by a thick interval of salt. It consists of Barremian to Aptian lacustrine carbonates with high permeabilities mainly due to high fracture intensities and carbonate dissolution, confirming large presence of fractures, karstification, and outstanding reservoir productivity (Correa et al., 2019). According to Akbar et al., 2001, hydrocarbon reservoirs in carbonate formations comprise nearly 50% of known economic reserves worldwide and most of them comprising naturally fractured reservoirs, as it is observed in some Brazilian pre-salt reservoirs (Correa et al., 2019). Therefore, a detailed knowledge of the fractures in these deposits will give a better understanding of their production behavior and development.

Open and uncemented or partially mineralized fractures often have a positive effect on oil flow, these can help to generate secondary porosity allowing communication between reservoir compartments (Aguilera, 1995; Bratton et al., 2006). In this way, fracture detection and evaluation (type, frequency, state, and orientation) are important for developing naturally fractured reservoirs (Khoshbakht et al., 2009; Ju et al., 2018). Moreover, the incorporation of fractures into reservoir models not only reduce the geological uncertainty for exploration, but also improve the forecast of production and guide the development plans (Correa et al., 2019).

Different data types can be used to describe fractures, including seismic data and attributes derived from it, geophysical logs, drill cores, and outcrops (Deng et al., 2015). According to (Sun et al., 2011), the combination of multiple seismic attributes is important for fault and

fracture detection since the coherence cube was first developed (Bahorich and Farmer, 1995), in addition, other algorithms were developed to improve the quality of images of faults and fractures such as curvature (Roberts, 2001), chaos (Schlumberger, 2009 in Gomez, 2018), and the “ant tracking algorithm” (Pedersen et al., 2003), the latter is widely used to enhance the resolution of the faults and fractures. However, despite the recent advances in three-dimensional seismic reflection techniques and in seismic attribute processing (Dorn, 1998), seismic data have limited resolution (Maerten L. and Maerten F., 2006). Therefore, the primary specialized tools for fracture detection are high-resolution image logs (Huapeng Niu et al., 2019), this is due to their optimal vertical resolution that, with almost full wall coverage of the boreholes, can assure that no features are missed along the borehole (Veltman et al., 2012).

Therefore, this work uses seismic attributes, as a big-scale tool to detect faults and large fractures, the method applied to delineate the faults was based on the Variance, Chaos and Ant-tracking (Appendix 2) volumes as important attributes to enhance discontinuity of seismic events. On the other hand, the image logs (Appendix 1) are used as a small-scale tool for in-situ stress determination and fracture detection and characterization; and as the production and development of a naturally fractured reservoir is highly influenced by the characteristics of the fracture network which may control the flow direction and volume of the hydrocarbons through the layers (Valentini et al., 2007), the primary goal of this research is to develop a DFN model based on the distribution of fractures in a geological grid in the reservoir, through the integration of image log, seismic attribute analysis, and supervised neural networks, which are the main tools for fracture mapping (Deng et al., 2015; Huapeng Niu et al., 2019), this models may help to improve the geological understanding of the Brazilian pre-salt section by providing information on high permeability regions for the evaluation of oil and gas accumulations.

Article 1: FRACTURE CHARACTERIZATION AND IN-SITU STRESS DETERMINATION USING BOREHOLE IMAGE LOGS AND SEISMIC DATA: THE PRE-SALT SECTION OF THE SANTOS BASIN, BRAZIL

ABSTRACT

The giant hydrocarbon accumulations discovered in the Brazilian offshore basins underneath the salt layer have opened a new exploratory frontier. The reservoir is mainly composed of naturally fractured lacustrine carbonates. Therefore, the understanding of natural fractures in these units provide insight of their geomechanical behavior, helping to optimize the potential and productivity of the reservoirs. One of the most used tools for reservoir characterization is the integration of the borehole image logs and seismic data. Accordingly, in this work, we used borehole image logs of 4 wells, and 3D seismic data to describe and interpret fractures and the in-situ stress state in the pre-salt play of the Santos Basin. The borehole breakouts and drilling-induced fractures were used as evidence to estimate a maximum horizontal stress (SH_{max}) with azimuth NE-SW; further, by comparing with the orientation and regime of large seismic scale structures in the reservoir, it is possible to highlight that the study area reveals a NE-SW normal fault pattern influenced by extensional stress configuration. Open natural fractures comprise four sets, the main sets with a greater abundance of fractures with strike NE-SW and the second sets of fractures with a lower prevalence in the study area with strike NW-SE. Outputs from this work can be used to constrain and build discrete fracture network models, which will allow to rank regions with enhanced fracture porosity and permeability, generating a view of preferential fluid flow paths in the reservoir.

INTRODUCTION

Understanding and characterizing naturally fractured reservoirs presents significant opportunities for the petroleum industry because they can be extremely profitable if managed correctly. This assumption has proved crucial in the development of fractured fields around the world, where faults and fractured zones have a significant impact on permeability and the development strategy is based on targeting of the discontinuities (Gutierrez, 2016). Thus,

predicting optimal flow routes requires a thorough understanding of the discontinuities in terms of intensity, orientation, and spatial distribution (Meldahl et al., 2001; Ligtenberg 2005).

The pre-salt reservoir of Santos Basin is positioned in the SE offshore continental margin of Brazil (Figure 1) in a sequence of Barremian to Aptian lacustrine carbonates, with a tectonic framework consisting of horsts and grabens associated with a faulting regime with normal component and transfer faults (Ojeda, 1982; Chang et al., 1992; Gomes et al., 2008). This carbonate sequence present high permeability owing to significant fracture intensities and carbonate dissolution, demonstrating the occurrence of fractures and karstification (Correa et al., 2019). In these carbonate reservoirs, fracture control parameters such as type, orientation, and intensity are essentially structural mechanisms, and they aid in understanding the complexity and variety of fractured reservoirs (Ghosh and Mitra, 2009); in addition, highlight fracture connectivity's contribution to flow regulation (Gong and Rossen, 2018).

Accordingly, this study utilizes seismic attributes, dedicated to detect faults and large fractures, and image logs as a tool for fracture detection, to determine the in-situ stress by interpreting the Breakouts and Drilling Induced Fracture and perform the fractures characterization by separating the types of natural fractures, with the goal of providing input for the development of a DFN model based on fracture distribution in the reservoir in order to better geological knowledge of the Brazilian pre-salt section.

GEOLOGICAL SETTING

The offshore Santos Basin locates in the Brazilian southeast coast and covers an area of ~ 350,000 km². Tectonically, the Santos Basin is a passive margin, limited to the north by the Campos Basin, separated by the Cabo Frio structural high, and to the south limited by the Pelotas Basin, separated by the Florianopolis structural high (Figure 1) (Moreira et al., 2007).

The basin presents a tectonic framework following a NNE-SSW trend, consisting of horsts and grabens associated with normal and transfer fault structures (Ojeda, 1982; Chang et al., 1992; Gomes et al., 2008). The tectonic history and evolution of the basin is associated to the rupture processes of the Gondwana supercontinent in the Jurassic-Cretaceous, which resulted in the

continental separation between west Africa and South America (Cainelli and Mohriak, 1999; Milani et al., 2000; Zalán et al., 2004).

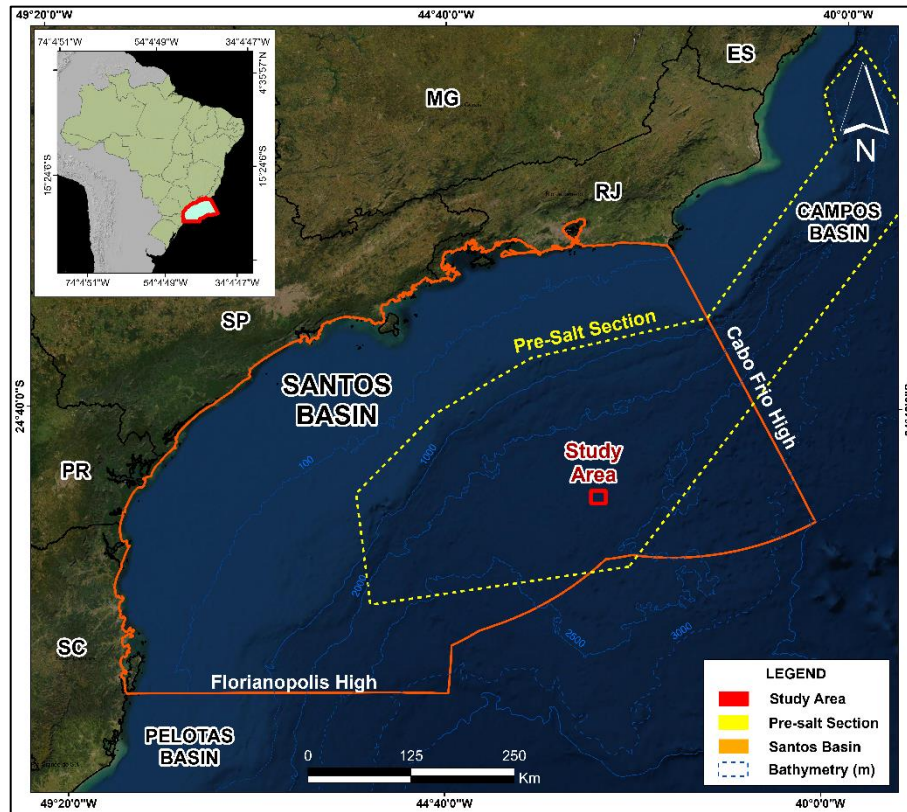


Figure 1. Location map of the study area and the Brazilian pre-salt section, situated in the SE offshore continental margin of the Santos basins. (Shapefiles taken from the Brazilian National Agency for Petroleum, Natural Gas and Biofuels, ANP).

The tectonostratigraphic evolution of the Santos Basin can be divided into three main super-sequences, rift, post-rift, and drift, each of these sequences bounded by regional unconformities (Pereira y Macedo, 1990; Pereira y Feijó, 1994; Moreira et al., 2007; Davison et al., 2012). This work is focused on the rift and post-rift super-sequences, for which the sedimentary record begins in the Hauterivian and extends up to the Aptian (Figure 2).

The rift phase is composed of basaltic flows defined as the Camboriu Formation, which its upper limit is an unconformity with the Picarras Formation. The Picarras Formation is composed of alluvial fans made up by conglomerates and sandstones in the proximal portions, and by lacustrine siltstones and shales in the distal portion. The upper part of the rift phase corresponds to the Itapema Formation, this is dominated by organic-rich carbonates, recognized by the abundant presence of rudstone and bivalves. The Itapema Formation is considered the

main source rock of the pre-salt play and its upper limit is demarcated by the pre-Alagoas unconformity, which marks the limit between the Itapema and Barra Velha formations (Moreira et al., 2007).

The post-rift phase includes the sag succession of the Barra Velha and the evaporites of the Ariri formations, deposited in transitional environments between continental and shallow marine (Moreira et al., 2007). The Barra Velha Formation is divided into Barra Velha Inferior and Barra Velha Superior, being these two separated by the Intra-Alagoas unconformity, which marks the beginning of the Sag phase (Wright and Barnett, 2015). The Barra Velha Formation is composed mainly of limestone, shales and high-magnesium claystones associated with in situ carbonates, formed in a hyperalkaline continental-marine transitional system (Moreira et al., 2007). The upper part of the post-rift phase corresponds to the evaporitic deposits (halite and anhydrite) of the Ariri Formation, and locally with the presence of soluble salts, such as tachyhydrite, carnalite and sylvinite (Amaral et al., 2015).

In summary, elements of the pre-salt petroleum system within the Santos Basin comprises a lacustrine source rock, a widespread and thick carbonate reservoir, and a thick salt interval acting as seal; the accommodation space for sedimentation was generated from the subsidence related to the distensible stresses that resulted in the Gondwana rupture (Moreira et al., 2007).

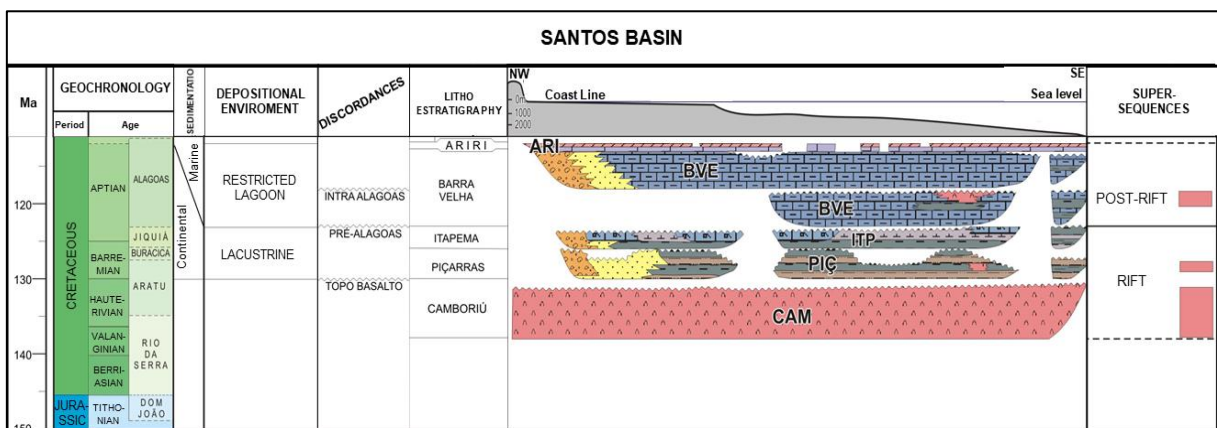


Figure 2. Lithostratigraphic chart of the rift and post-rift super-sequences of the Santos Basin. (Extracted from Moreira et al., 2007).

DATABASE

The data was acquired from the ANP repository (National Agency for Petroleum, Natural Gas and Biofuels) and comprise a seismic volume along with well information. The volume contains a 3-D post-stack time migrated seismic of 300 km², it covers 650 inlines and 700 crosslines with an interval spacing of 12.5x12.5 m. The recording interval was 8000 ms with a sampling rate of 4 milliseconds. The well information includes check-shots, formation tops, sonic logs, density logs and borehole image logs from 4 wells, which include fracture point data such as dip angle, dip azimuth and fracture type (natural vs induced).

METHODS

Horizons and Faults Interpretation

Prior to seismic interpretation, the seismic volume was preconditioned, involving noise removal to increase the signal-to-noise ratio and obtain better continuity of the reflectors. In addition, different seismic attributes were used to emphasize discontinuities and, as a result, highlight possible faults (Figure 3).

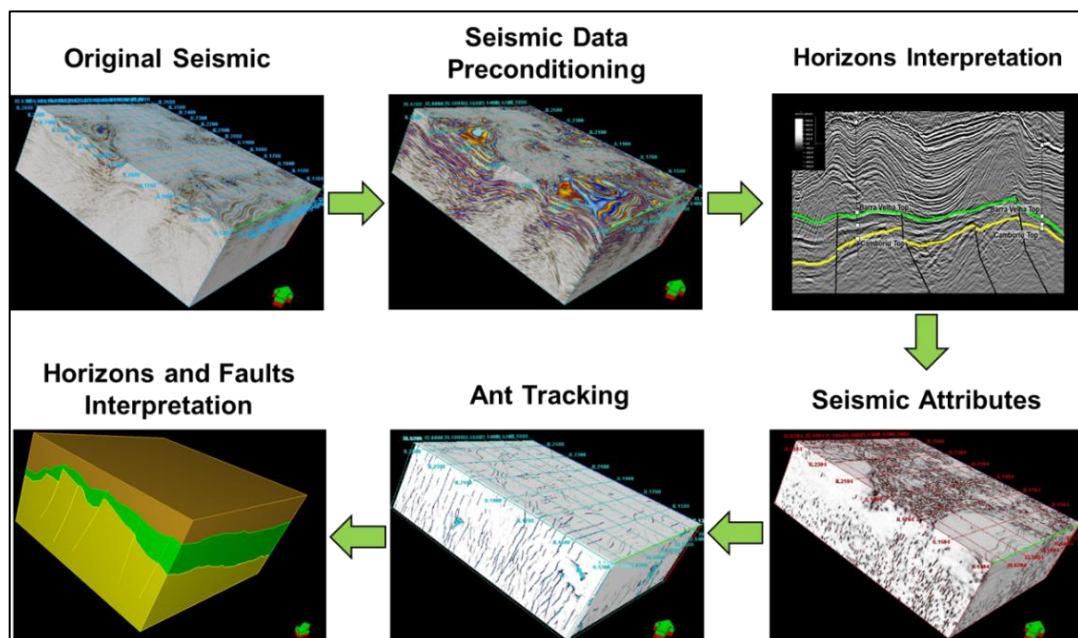


Figure 3. Workflow used to highlight faults and discontinuities from seismic attributes. Results illustrate the interpreted horizons and intersections with faults.

The preconditioning of the seismic volume was based upon applying filters to eliminate seismic anomalies, such as acquisition footprints or multiples. Initially, a semi-automated geostatistical filter (Destriping Filter) was applied, which once the parameters (noise orientation, the noise/signal variability, and the noise distribution) have been established, factorial kriging filters out the noise using local noise and signal characteristics (Magneron et al., 2009). Subsequently, the structure-oriented filter (SOF) is executed, which removes the random noise by aligning the seismic reflector using the dip-steering principle, thus improving the structural and stratigraphic characteristics of the data (Chopra and Marfurt, 2008). Lastly the Dip Steered Median Filter (DSMF) is applied which adjusts the diffuse terminations of the reflectors closer to the fault zones with a pre-computed geometry attribute, which identifies the dissimilar seismic traces and improves the edge of the reflectors (Jaglan and Qayyum, 2015) (Figure 4).

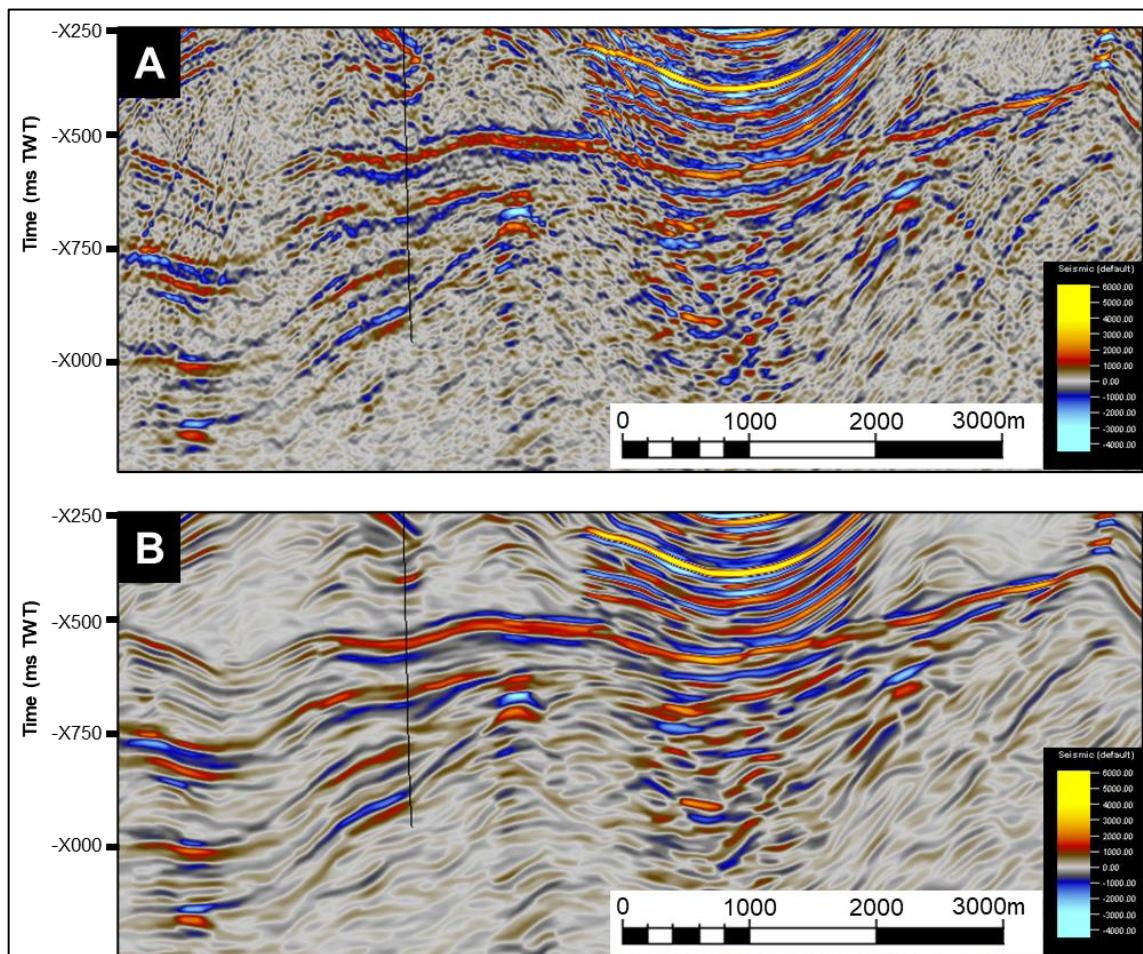


Figure 4. Seismic cross-section showing the noise-reduction filter. (A) Original seismic. (B) After dip steered median filter (DSMF).

Following the application of noise-reduction filters to improve the data's structural and stratigraphic features, two main horizons were interpreted, including the base of the salt (representing the top of the pre-salt play) and the base of the pre-salt play (representing the top of the Camboriu Formation) that are identified as a high positive impedance using the correlation between the seismic and the well markers.

Post data conditioning, multiple seismic attributes such as variance, chaos and ant tracking were executed to highlight discontinuities and consequently identify possible faults. Variance attribute is a measure of the similarity between the seismic traces. Geologically, high coherence waveforms indicate lateral lithological continuity, while abrupt coherence changes can suggest faults and large fractures. Its main utility is the ability to enhance discontinuities, allowing the precise interpretation of fault lineaments (Chopra & Marfurt, 2007). The Chaos attribute is an edge detection method and computes the local chaos – measure of the ‘lack of organization’ in the dip and azimuth estimation method. It can also be used to enhance faults and discontinuities (Schlumberger, 2009 in Gomez, 2018). The Ant Tracking algorithm is part of an innovative workflow that introduces a new paradigm in fault interpretation, this emulates the behavior of ant colonies in nature and how they use pheromones to mark their paths in order to optimize the search for food. Similarly, virtual ants are put as ‘seeds’ on a seismic discontinuity volume to look for fault zones. Virtual pheromones deployed by the ants capture information related to the fault zones in the volume. The result is an attribute volume that shows very sharp and detailed fault zones, since it better enhances horizon discontinuities when compared to other traditional edge enhancing attributes (Chaos, Variance) (Silva et al., 2005) (Figure 5).

From the application of the seismic attributes and filters aforementioned, which are dedicated to enhancing the discontinuities, the interpretation of main faults of the pre-salt play was possible consisted of locating the fault planes in different seismic sections, taking into account the interruption or change of continuity of the reflectors or seismic horizons already interpreted.

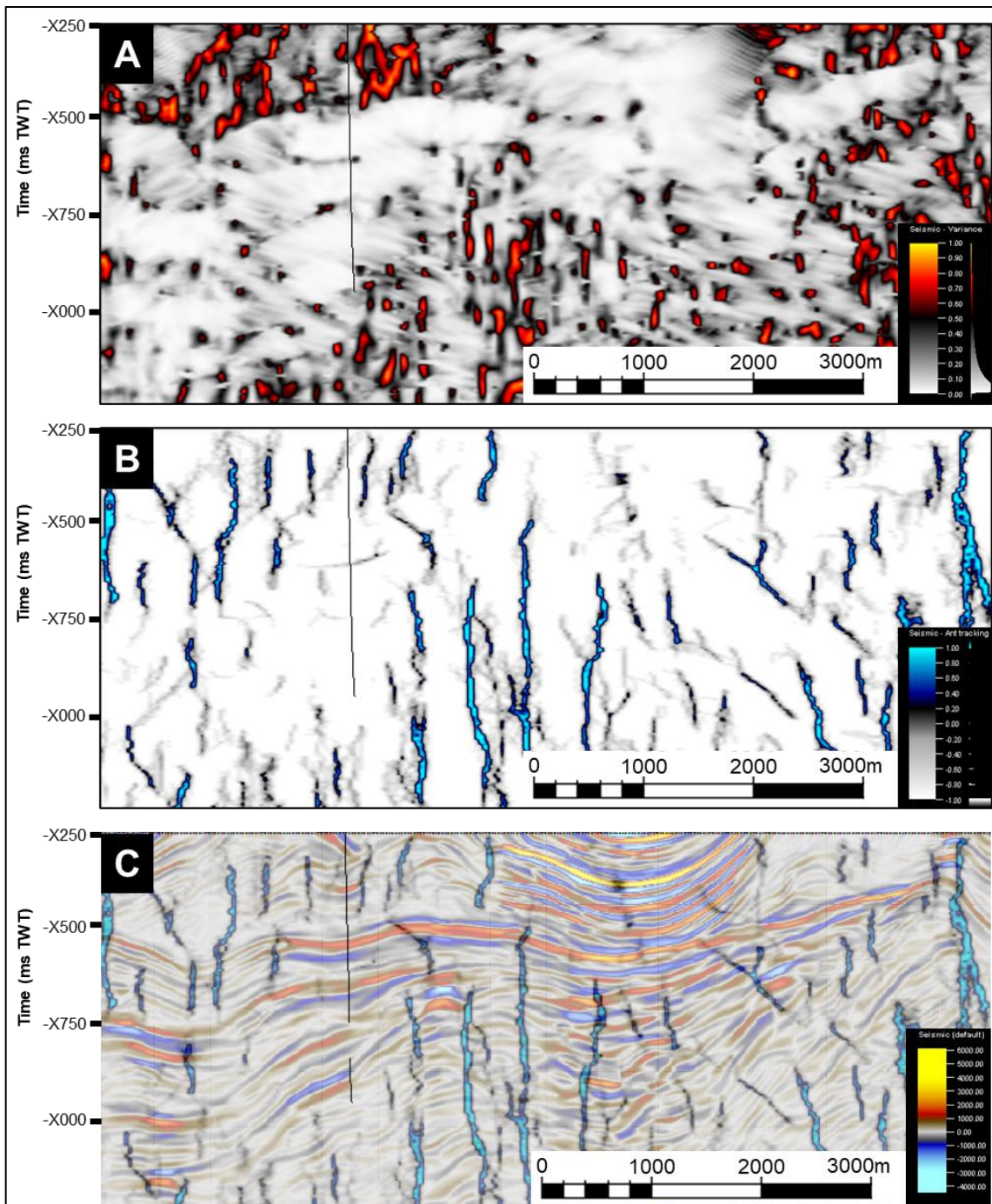


Figure 5. Seismic attributes executed to highlight discontinuities. (A) Variance. (B) Ant tracking. (C) Ant tracking overlaid with original seismic.

Borehole Image Logs

Borehole images are a powerful tool for structural and sedimentological interpretation that allows the obtention of dip and azimuths of faults, fractures and sedimentary structures from borehole wall (Haller and Porturas, 1998; Khoshbakht et al., 2012; Kingdon et al., 2016; Brekke et al., 2017; Lai et al., 2019). In this work, the data was loaded and interpreted according to the

available tool from each well and calibrated according to magnetic declination and accelerometer to provide the true orientation of interpreted structures. The interpretations were carried out by acoustic tools acquired from Circumferential Acoustic Scanning (CAST tool of Halliburton) or Ultrasonic Borehole Imager (UBI tool of Schlumberger). Both tools are capable to generate a 360° image of the borehole wall and provides good image resolution for the interpretation of natural and drilling induced fractures as well as the breakouts of borehole wall (Abdideh and Amanipoor, 2012; Kingdon et al., 2016). The differences between Natural Fracture (NF) and Drilling Induced Fracture (DIF) are associated with their origin, the first occur in subsurface as a result of geological process and the latter is a result of a regional stress of the field centered around of borehole wall during drilling. Both fractures can be distinguished in acoustic borehole images according their geometries and trace. In case of vertical or sub-vertical wells, like our dataset, the DIF exhibit a sub-parallel or slight inclined orientation to the borehole axis, developed closely to the maximum stress orientation. Generally, they do not fully cross the wellbore and exhibit an asymmetrical distribution, whereas the NF have a consistent orientation and are often symmetrically along the full wellbore section (Figure 6).

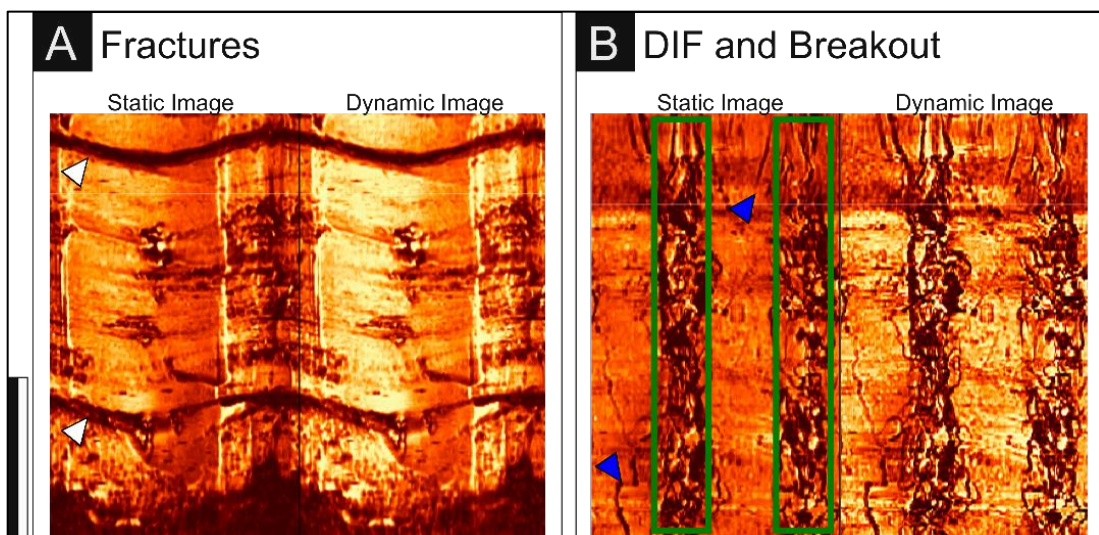


Figure 6. Visualization of natural fractures, drilling induced fractures and breakouts in acoustic borehole images. A) Occurrences of open and enlarged natural fracture pointed by the white arrow and B) Irregular and vertical drilling induced fractures pointed by the blue arrow and breakouts highlighted in green area. Note that natural fractures have lateral continuity while DIF are irregular and vertically arranged, furthermore the DIF are arranged 90° of the orientation of breakouts.

For the in-situ stress analysis it is necessary to take into account that the in situ stress is the sum of all natural stress contributions and natural processes that influence the rock stress state at a given point; it also refers to the current natural stress related to the tectonic and gravitational forces; assuming that the vertical stress (S_v) is a principal stress at depth, the orientation of the maximum (S_{Hmax}) and minimum (S_{Hmin}) horizontal stress are the other two principal stresses of the stress tensor (Heidbach et al., 2016) (Figure 7A) and these can be determined from breakouts and drilling-induced fractures, where the S_{Hmax} is approximately perpendicular to the breakouts, and parallel to drilling-induced fractures (Plumb and Hickman, 1985) (Figure 7B).

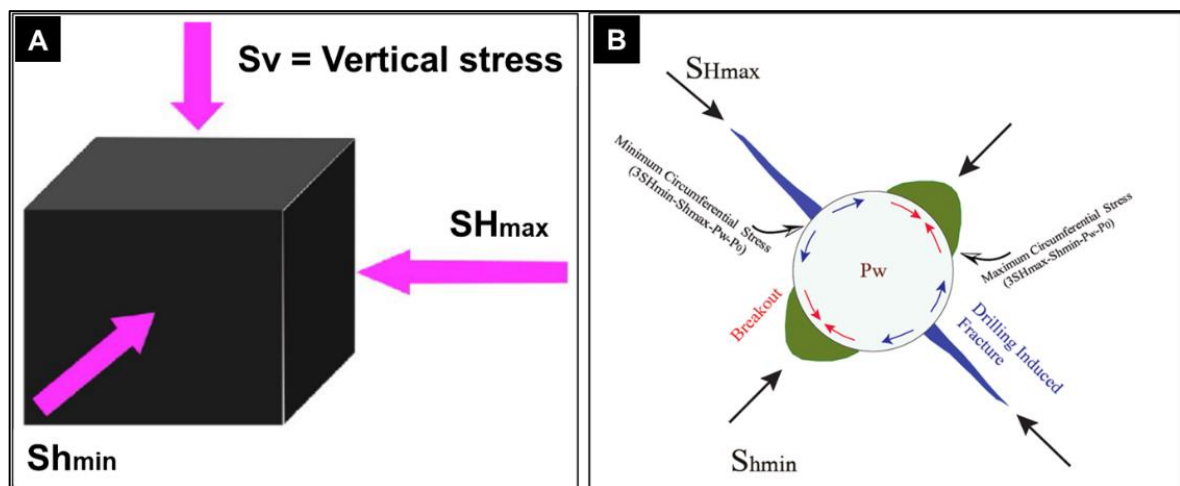


Figure 7. A) In-situ stress state is defined by: vertical stress (S_v), maximum principal horizontal stress (S_{Hmax}) and minimum principal horizontal stress (S_{Hmin}) (Extracted from Hupeng Niu et al., 2019). B) Typical borehole breakout and drilling-induced fractures. The S_{Hmax} is approximately perpendicular to the breakouts, and parallel to drilling-induced fractures (Extracted from H. Talebi et al., 2018).

Finally, all dips and azimuths were plotted in rose diagrams to display breakout and fracture data, through which the maximum/minimum horizontal in-situ stress are determined; as well as the definition of main fracture sets (Figure 8).

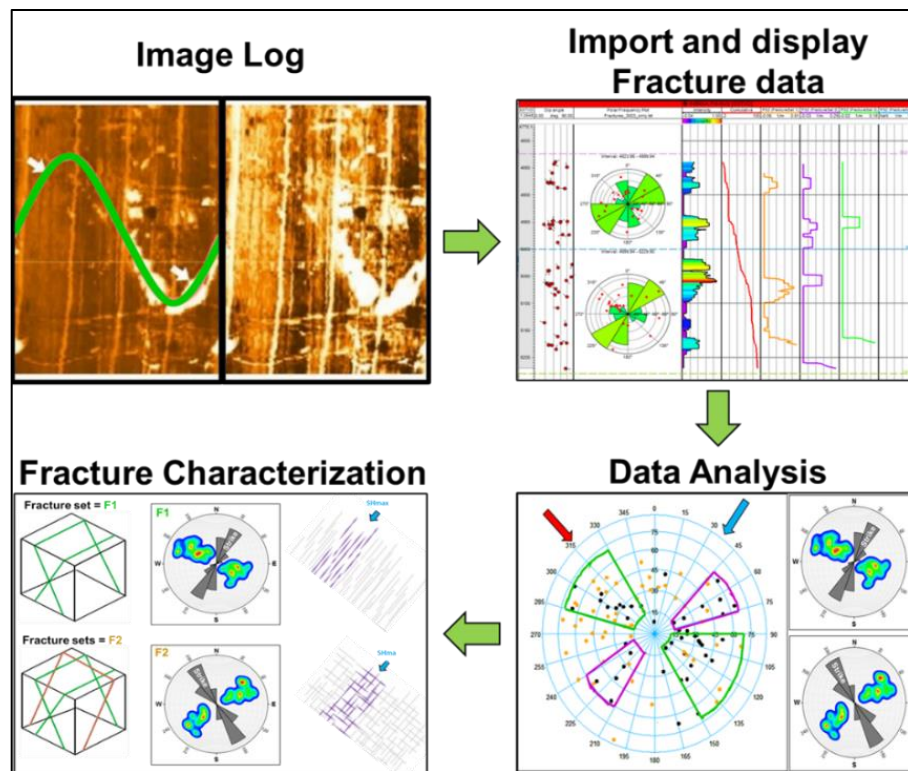


Figure 8. Workflow used to fracture characterization from borehole image logs.

RESULTS AND DISCUSSION

Seismic Interpretation (Horizons and Faults)

The seismic interpretation was focused on the identification of the main horizons (top and base of the pre-salt play) and regional faults of the study area. Figure 9 and Figure 10 shows the identified horizons (Barra Velha and Camboriu formations tops) and the regional structural configuration. The top of the pre-salt play was mainly observed as a continuous reflector, it presents a strong change between the sediments of the Barra Velha Formation and the salt of the Ariri Formation, which presents some distortions or chaotic patterns due to the effects of the salt, allowing an enhancement of its base reflector making it easy to identify (Figure 9C and Figure 10C). The Camboriu Formation top was mainly identified by the typical chaotic reflections of the basement, which generate a strong change between the basalts and the sedimentary rocks of the pre-salt play (Figure 9C and Figure 10C). This strong change is also seen in the well logs, mainly in the sonic log, which is one of the best indicators due to the drastic contrast in transit times between the pre-salt play with the salt and the basement (Figure 9D and Figure 10D).

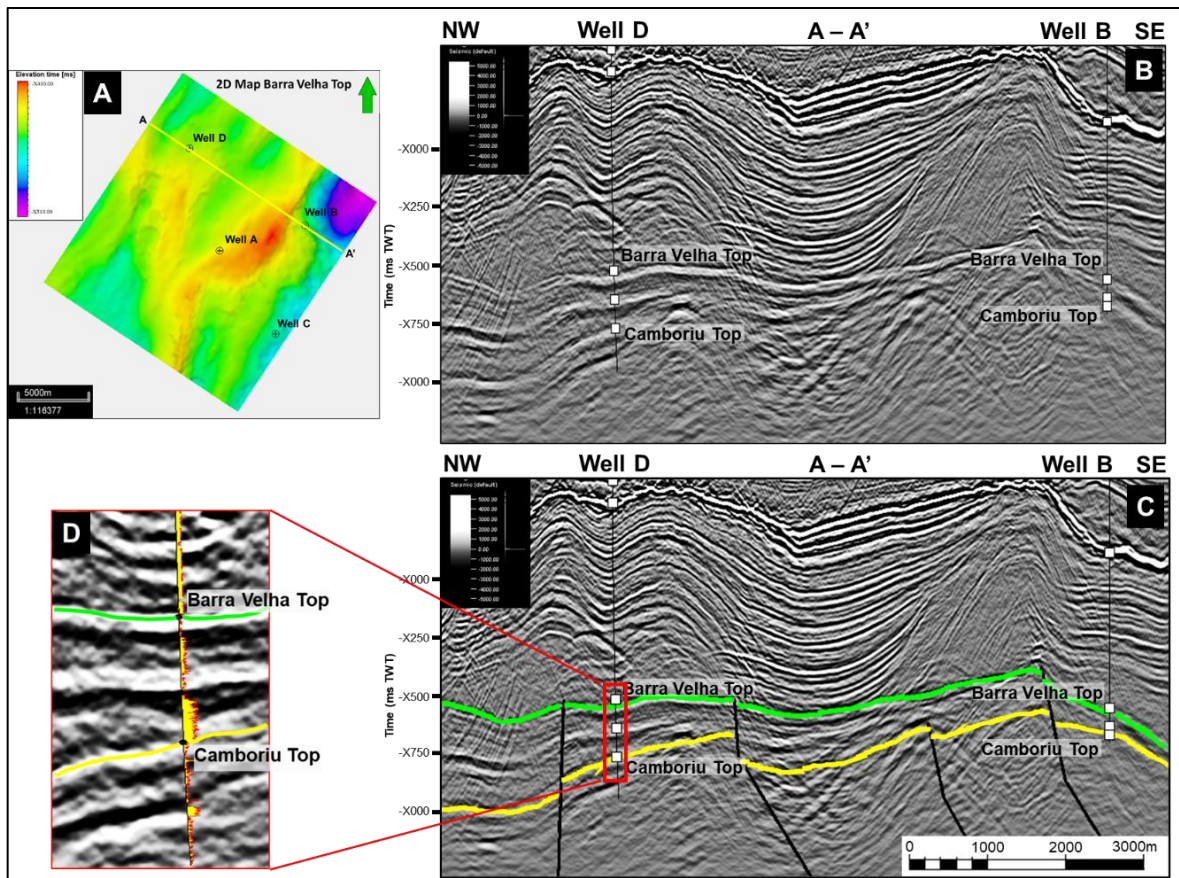


Figure 9. A) 2D map of the Barra Velha Formation top surface. Showing the seismic cross section (A-A') on the yellow line. B) Seismic cross section (A-A') before interpretation. C) Interpreted seismic section (A-A') of the main horizons (top and base of the pre-salt play, green and yellow lines respectively) and regional faults (black lines) of the study area. D) Zooming in on the intersection of the sonic log (Well D) with the seismic, showing the strong change between the interpreted horizons, the salt and the basement.

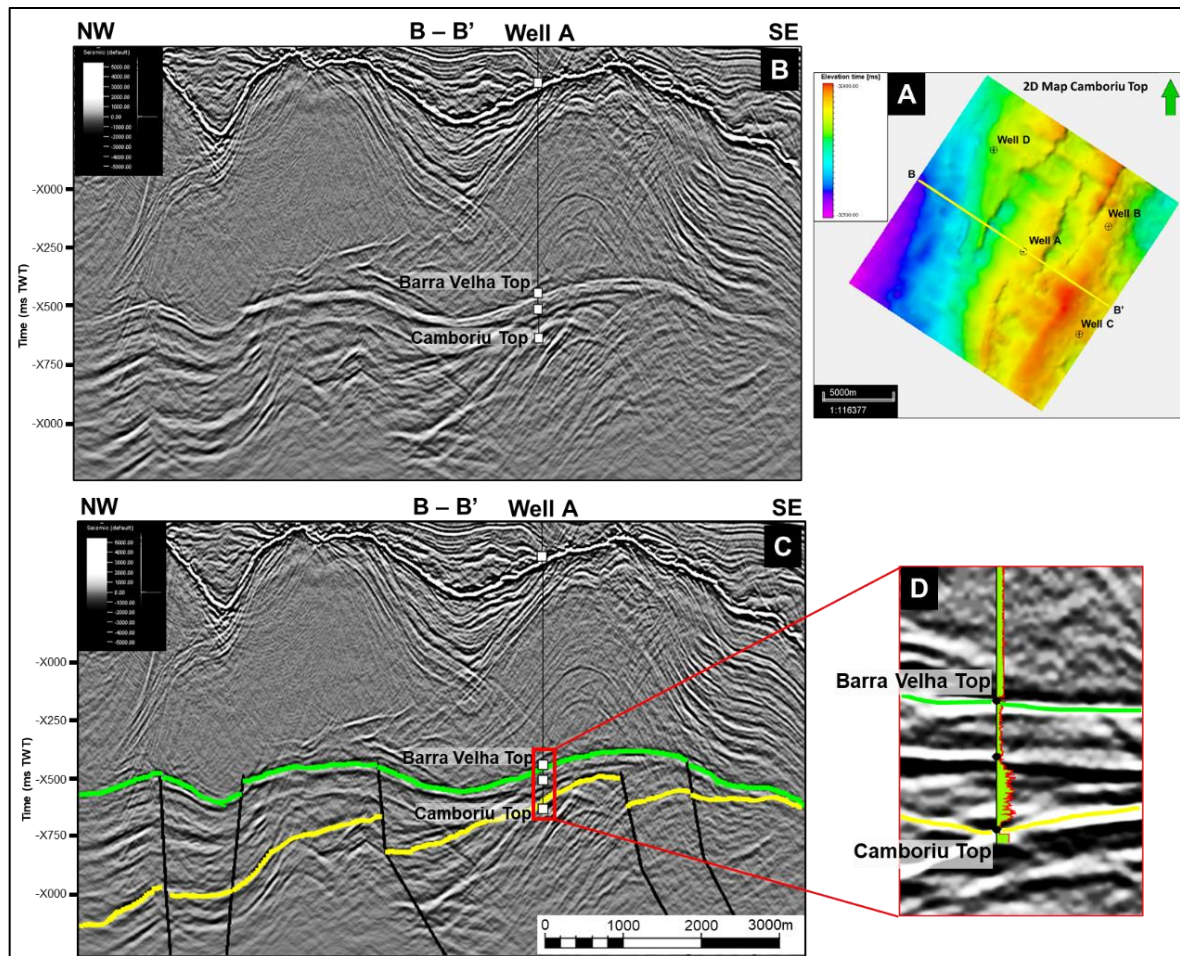


Figure 10. A) 2D map of the Camboriu Formation top surface. Showing the seismic cross section (B-B') on the yellow line. B) Seismic cross section (B-B') before interpretation. C) Interpreted seismic section (B-B') of the main horizons (top and base of the pre-salt play, green and yellow lines respectively) and regional faults (black lines) of the study area. D) Zooming in on the intersection of the sonic log (Well A) with the seismic, showing the strong change between the interpreted horizons, the salt and the basement.

The interpretation of main faults in the pre-salt play was carried using results from seismic attributes such as chaos, variance and ant tracking, all of which enhancing discontinuities and allowing visualization of the regional structures. According to this interpretation, the regional structural framework of the pre-salt play in the study area is characterized by normal faulting, and the general orientation of the interpreted faults follow a main strike NE-SW (Figure 11), this most likely related to the rupture of the Gondwana supercontinent in the Jurassic-Cretaceous period and the continental separation between Africa and South America (Ojeda, 1982; Chang et al., 1992; Cainelli and Mohriak, 1999; Milani et al., 2000; Zalán et al., 2004).

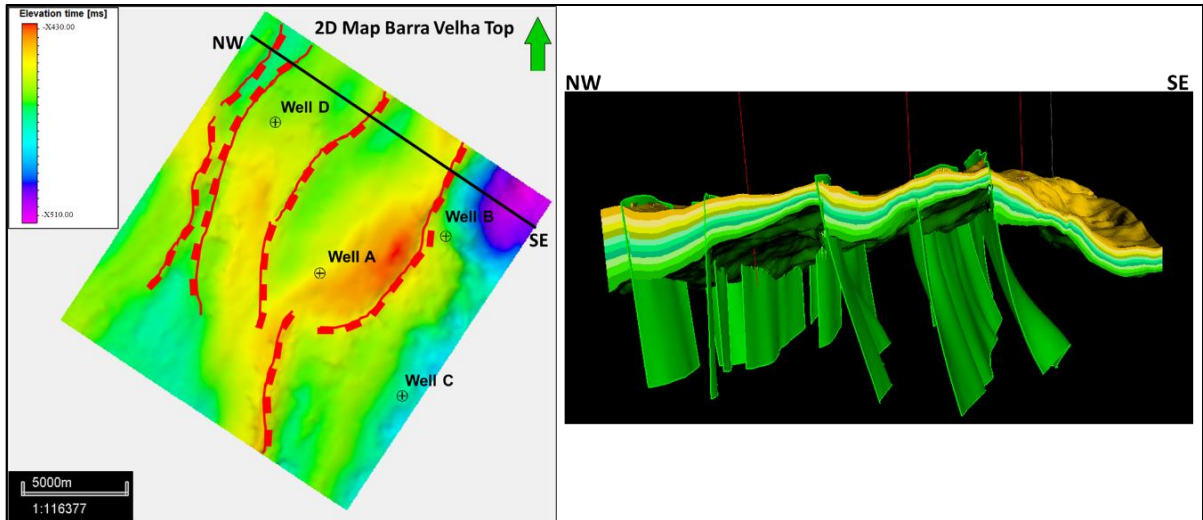


Figure 11. Regional structural framework of the pre-salt play in the study area characterized by high-angle normal faulting.

Interpretation and analysis of breakouts and drilling-induced fractures (In-situ stress analysis)

The analysis of the breakouts and drilling-induced fractures was performed jointly for the four wells. According to the interpretation, 41 breakouts and 25 drilling-induced fractures in the pre-salt play were identified covering the information from 4 wells.

Based on the expressed in the methodology, the breakouts are represented by continuous dark zones where the borehole wall was collapsed following the minimum horizontal stress (S_{hmin}) and the DIF exhibit a sub-parallel or slight inclined orientation to the borehole axis, developed closely to the maximum horizontal stress (S_{Hmax}) therefore, with what is observed in Figure 12, the average trend of breakouts develops through the NW-SE direction of the borehole, which can be considered as the S_{hmin} direction, and drilling-induced fractures are through the NE-SW direction, suggesting the S_{Hmax} follows that direction. Thus, the present-day maximum in-situ stress has a direction of NE-SW in the pre-salt play of the study area.

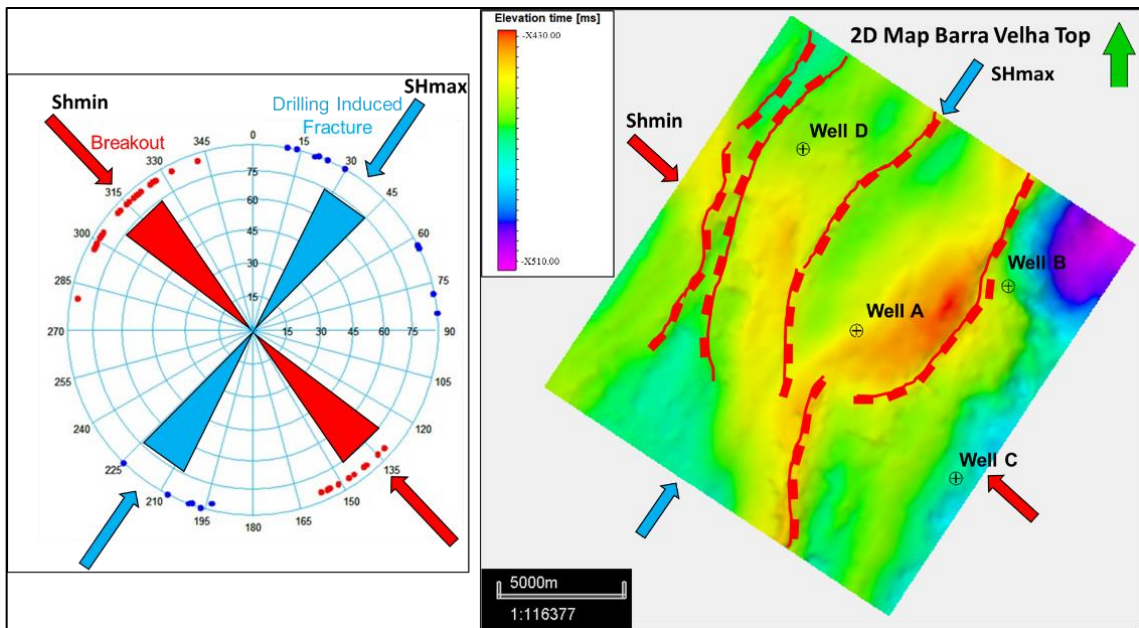


Figure 12. The orientation of the minimum horizontal stress (Shmin) and the maximum horizontal stress (SHmax) determined from the borehole breakout and drilling-induced fractures.

The analysis of breakouts and drilling-induced fractures obtained from the borehole image logs allowed the estimation of present-day maximum and minimum in situ stress directions of the pre-salt play in the study area, which are determined by a strike NE-SW for the SHmax (orthogonal to the breakouts) and NW-SE for the Shmin (parallel to the breakouts) (Figure 13A). Comparing this result of the present tectonic regime with the orientation and regime of the interpreted faults, it is possible to highlight that the study area is influenced by a normal stress configuration, defined by the relation $S_v > SH_{max} > Sh_{min}$ (Figure 13B), this according to the classification to describe a fault's movement at different stress states outlined by Anderson (1905), where a fault will slip normally when $S_v > SH > Sh$, and such a stress regime is considered "normal". Similarly, stress regimes that allow strike-slip fault movement $SH > S_v > Sh$ and reverse (or thrust) fault movement $SH > Sh > S_v$ (Shen et al., 2018) (Figure 13 B).

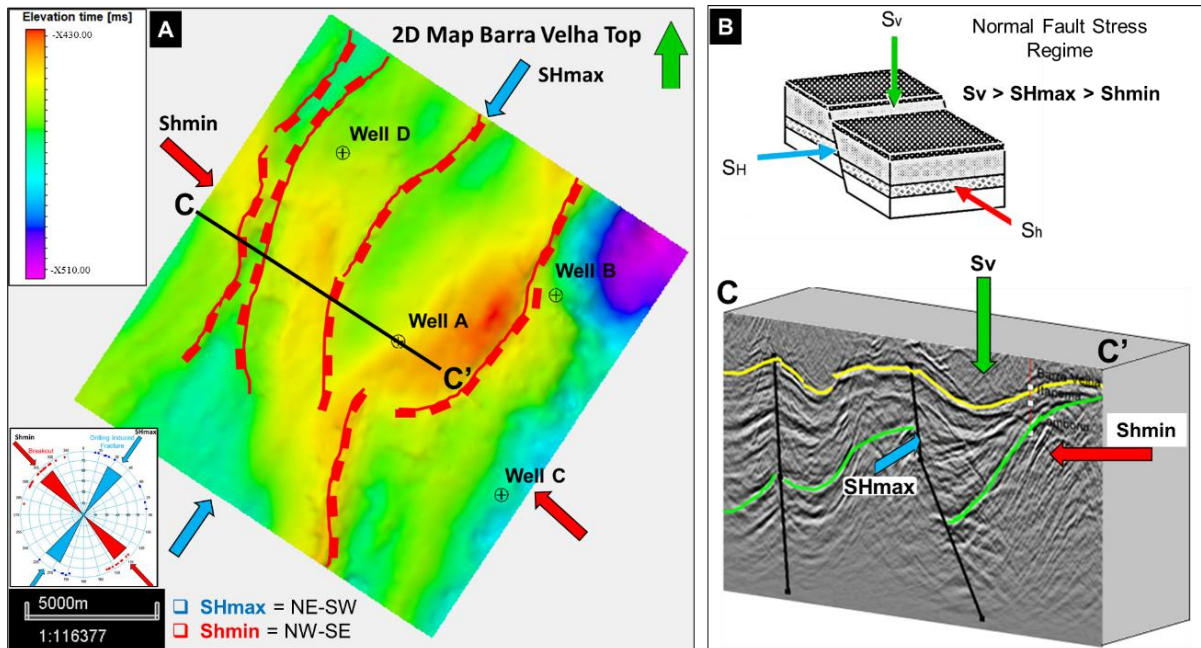


Figure 13. Maximum and minimum horizontal stress analysis. A) Demonstration of the structural configuration of the study area based on breakouts and drilling-induced fractures. B) Model that the study area is influenced by a normal stress configuration, defined by the relation $S_v > S_{Hmax} > S_{Hmin}$, according to normal fault stress regime (Anderson, 1905).

Interpretation and analysis of well fractures data

This analysis was based on the information of the dip angle and dip azimuth of the fractures interpreted in the well images. From results of interpreted fractures, it was possible to identify that the fractures in all wells show a dominant strike direction NE-SW with a preferential average dip inclination of 40 degrees, however, in wells B, C and D it is possible to identify a second less prominent strike direction NW-SE (Table 1, Figure 14 and Figure 15).

Table 1. Results of natural fractures identified in wells A, B, C and D.

WELL A		
Formation	Barra Velha	Itapema
Main Strike direction	N49E-S49W	N41E-S41W
Average dip inclination	40°	43°
WELL B		
Formation	Barra Velha	Itapema
Main Strike direction	N30E-S30W	N29E-S29W
	N42W-S42E	
Average dip inclination	36°	39°

WELL C		
Formation	Barra Velha	Itapema
Main Strike direction	N37E-S37W	N46E-S46W
		N42W-S42E
Average dip inclination	35°	46°
WELL D		
Formation	Barra Velha	Itapema
Main Strike direction	N45E-S45W	N28W-S28E
		N38E-S38W
Average dip inclination	45°	53°

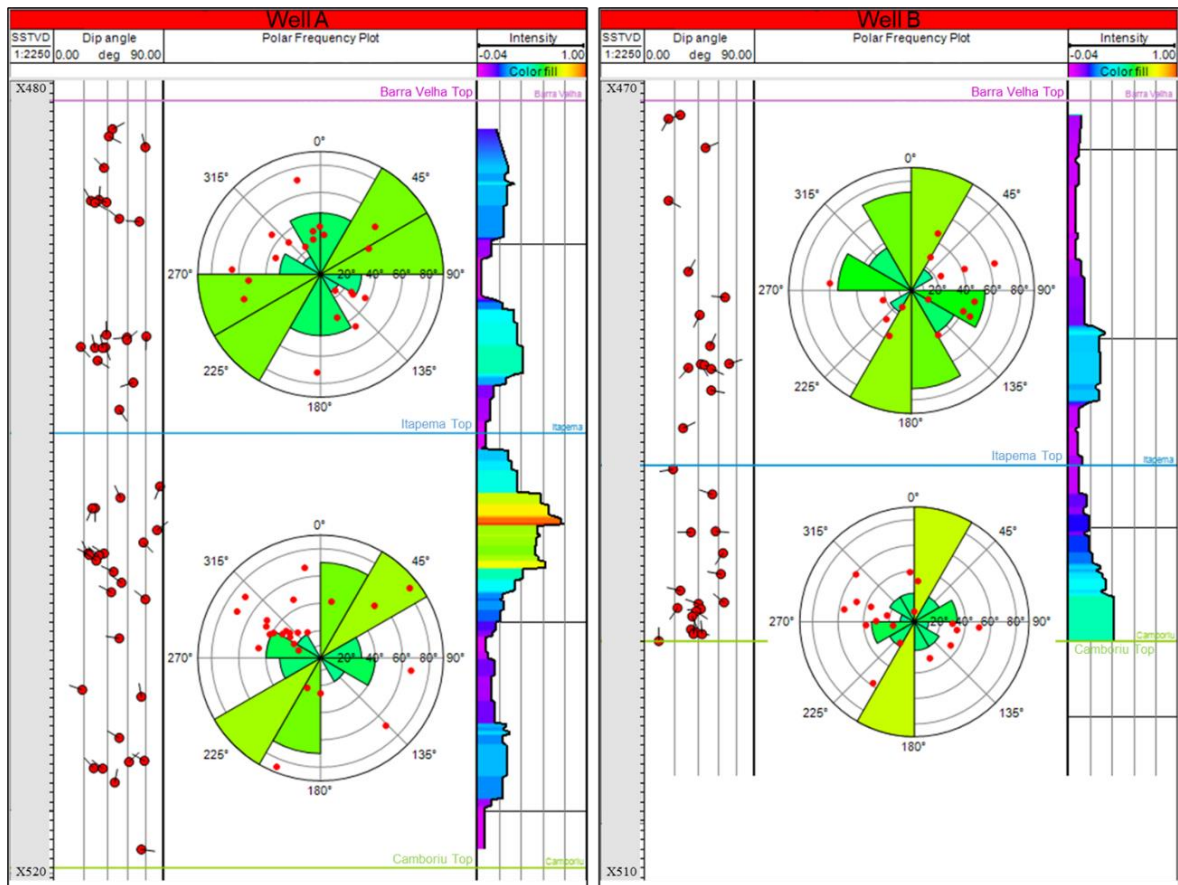


Figure 14. Fractures expressions and fracture intensity log of well A and Well B.

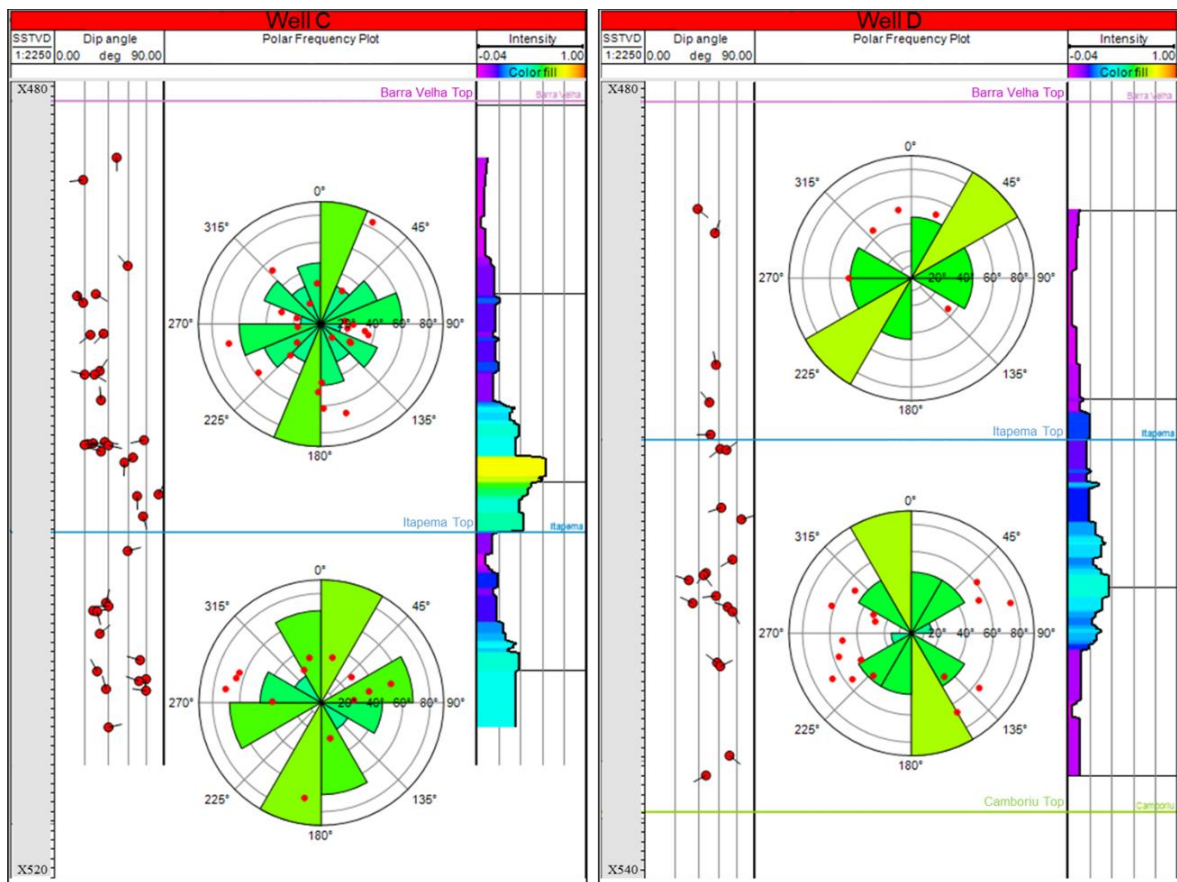


Figure 15. Fractures expressions and fracture intensity log of well C and Well D.

Results of the fractures observed for each well reveal two main sets of natural fractures dominating in all wells with a strike direction NE-SW and dip directions NW and SE (Figure 14 and Figure 15), this orientation correlates with the fault and large fracture patches extracted from the ant tracking attribute (Figure 16A), which were plotted in stereo net diagram and showed a prominent strike NE-SW (Figure 16B) and dip azimuths NW and SE (Figure 16BC). The analysis of breakouts and the natural fractures shows that the most abundant sets of natural fractures in the pre-salt play are approximately parallel to SHmax, suggesting for these fractures an open state (open fractures) and good connectivity, similar to observations by Huapeng Niu et al., 2019 in the Dongying Formation of the Bohay bay basin of China.

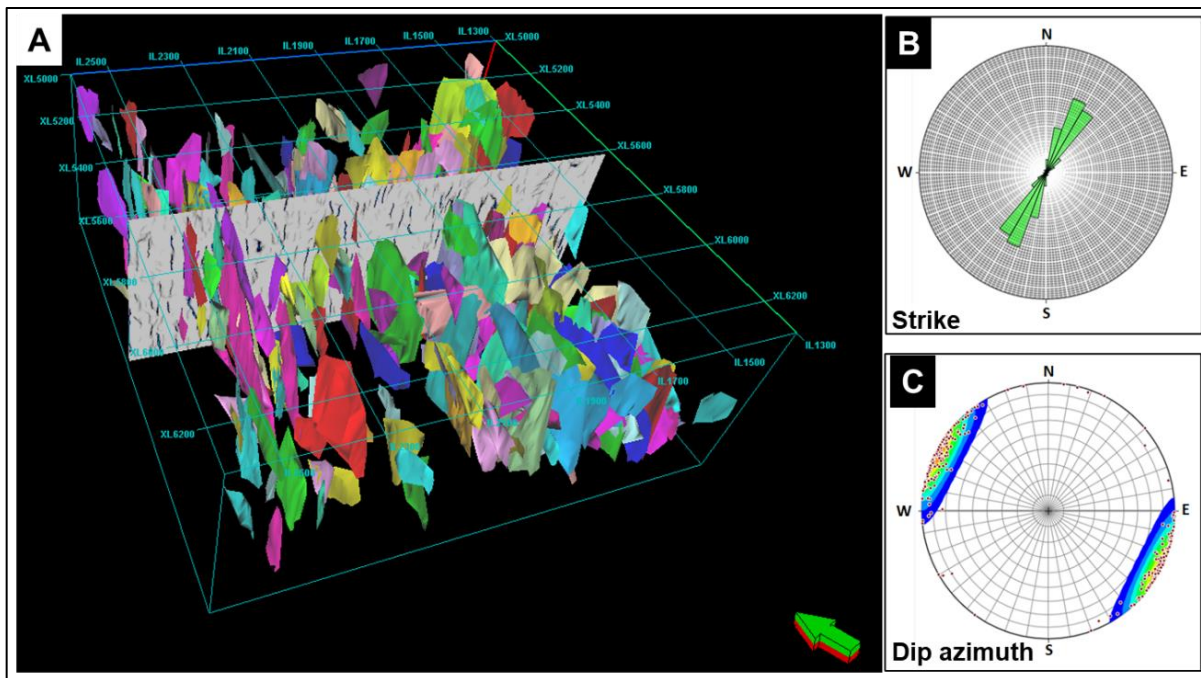


Figure 16. A) Fault and large fracture patches extracted by ant tracking algorithm, B) illustrating the prominent strike direction NE-SW on stereo net diagram. C) illustrating dip directions NW and SE.

Further, given the high connectivity that open fractures could represent at predicting the trajectory of reservoir fluid flow, a joint analysis of open fractures for the 4 wells was carried out, in order to evaluate potential intervals/zones for hydrocarbon production. According to this joint analysis (Figure 17 and Figure 18), four sets of fractures are recognized, two main sets with a greater abundance of fractures with a strike NE-SW (F1 and F2 follow a strike parallel to SHmax) and an average dip inclination of 45 and 37 degrees respectively, and the others two sets of fractures with a lower prevalence in the study area with a strike NW-SE (F3 and F4 follow a strike orthogonal to SHmax) with an average dip inclination of 53 and 43 degrees respectively.

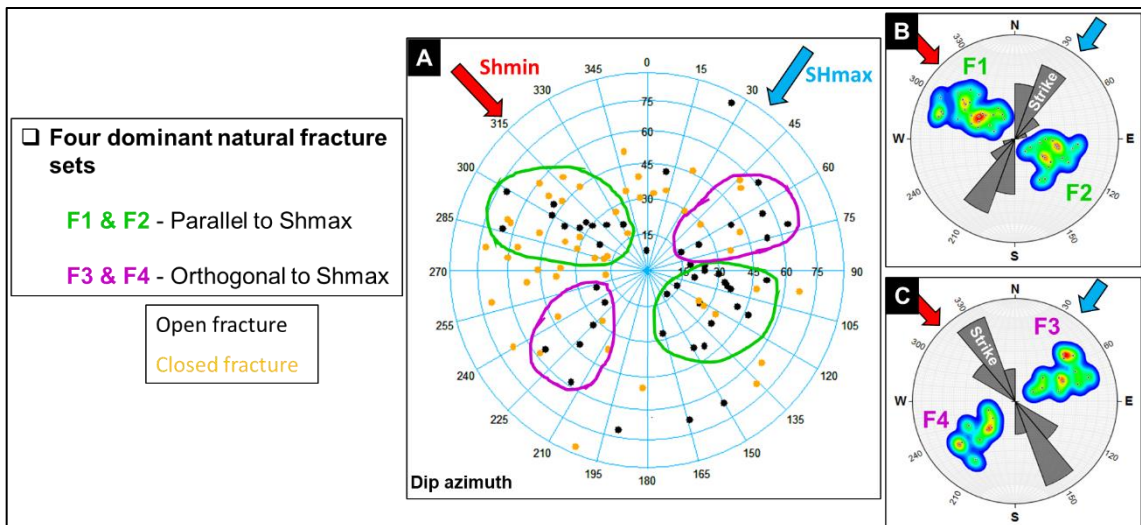


Figure 17. Evaluation of open and closed natural fractures. A) Illustrating four sets in the pre-salt play. stereo net diagram representing the Dip azimuth. B) Stereo net diagram highlighting the two main sets with a strike NE-SW parallel to SHmax. C) Stereo net diagram highlighting the two sets with a lower prevalence with a strike NW-SE orthogonal to SHmax.

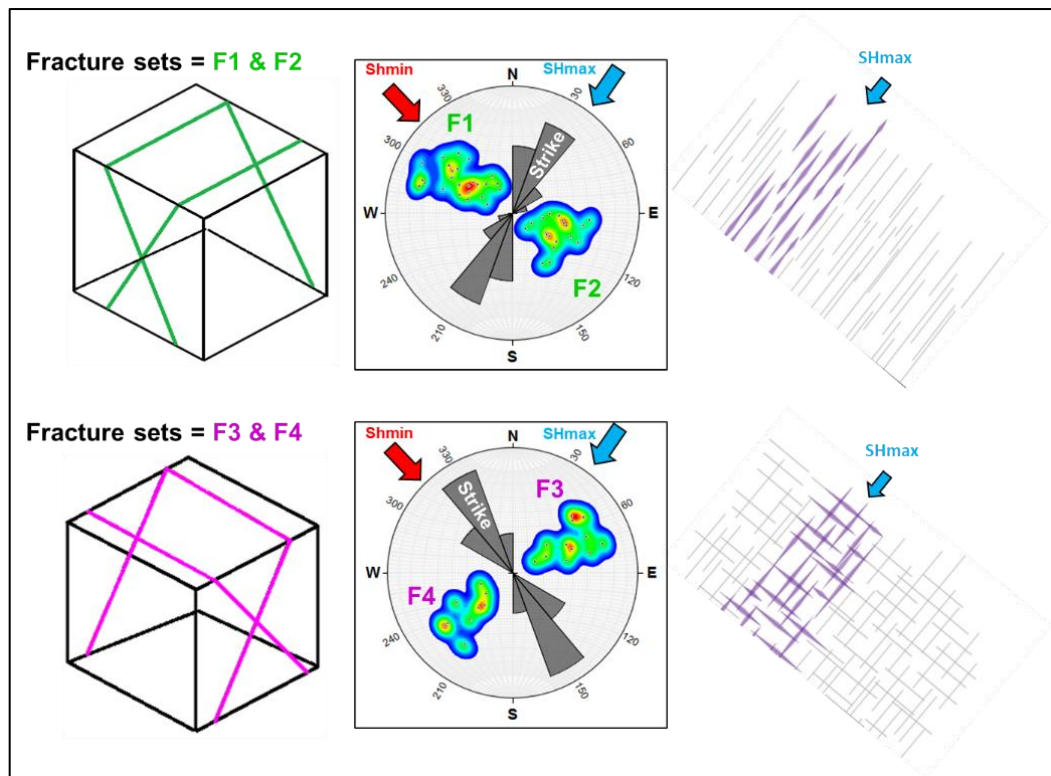


Figure 18. Summary plot of the main fracture sets identified in the pre-salt play from borehole image logs.

The set of fractures with a strike NE-SW develops in the same direction as the regional configuration of the study area, for which it is suggested that they are predominantly related to extensional faults and thus likely be formed by slight changes in the movements during the

hyper-extensive stage in the rifting process (Oliveira et al., 2019). And according to the fractures set with strike NW-SE, which has a less prominent and more local distribution in the study area, according to Morley et al., 1990, these fractures can be considered as parts of transference zones or accommodation zones between the faulted blocks.

CONCLUSIONS

With the mapping of the breakouts and drilling-induced fractures, it was possible to estimate the present maximum and minimum in situ stress directions of the pre-salt play in the study area, these directions are recognized by a strike NE-SW for the SHmax and NW-SE for the Shmin, influenced these two by a normal stress configuration.

Regarding the analysis of borehole image logs, the orientation of open fractures reveals the presences of four sets of fractures, two main sets with a greater abundance of fractures with a strike NE-SW that runs parallel to SHmax and two second sets of fractures with a lower prevalence with a strike NW-SE.

The seismic interpretation of the main horizons (top and base of the pre-salt play) and the regional faults of the study area is characterized by normal stress configuration that corroborate the present in-situ stress regime.

Outputs and observations from this work can be used to build discrete fracture network models, which will further allow to represent regions with high fracture porosity and permeability.

REFERENCES

- ABDIDEH, M., and AMANIPOOR, H., 2012. Fractures and Borehole Breakouts Analysis of a Reservoir Using an Image Log (Case Study: SW Iran). *Petroleum Science and Technology*, 30:22, 2360-2372. DOI: 10.1080/10916466.2010.512895.
- AGUILERA, R. 1995. *Naturally Fractured Reservoir*. Second edition. Tulsa, Oklahoma: PennWell Publishing Company. ISBN 0-87814-449-8

- AKBAR, M., VISSARPRAGADA, B., 2001. A Snapshot of Carbonate Reservoir Evaluation. *Oilfield Review*, 12, 20–41.
- AMARAL, P. J., MAUL, A. R., FALCÃO, L., CRUZ, N. M., GONZALEZ, M. A., & GONZÁLEZ, G., 2015. Estudo Estatístico da Velocidade Dos Sais Na Camada Evaporítica Na Bacia De Santos. 14th International Congress of the Brazilian Geophysical Society & EXPOGEF, Rio de Janeiro, Brazil, 3-6 August 2015. Brazilian Geophysical Society. p. 666-669.
- ANDERSON, E.M., 1905. The Dynamics of Faulting; *Transactions of the Edinburgh Geological Society*, v. 8, no. 3, p. 387–402.
- ARIZA, D., MOREIRA, W., DE ANDRADE, I., RODRIGUES, J., FERRARI, A., PIERANTONI, L. AND OLHO, M., 2019. Unsupervised Seismic Facies Classification Applied to a Pre-Salt Carbonate Reservoir, Santos Basin, Offshore Brazil. *AAPG Bulletin*, v. 103, no. 4 (April 2019), pp. 997–1012.
- BAHORICH, M.S., and FARMER, S.L., 1995, 3-D Seismic Discontinuity for Faults and Stratigraphic Features: The Coherence Cube: *SEG Expanded Abstract*, 93-96.
- BOURBIAUX, B., 2010. Fractured Reservoir Simulation: A Challenging and Rewarding Issue. *Oil and Gas Science and Technology – Revue de IFP*, 65, 227–238.
- BRATTON, T., VIET CANH, D., VAN QUE, N., DUC, N., GILLESPIE, P., HUNT, D., LI, B., MARCINEW, R., RAY, S., MONTARON, B., NELSON, R., SCHODERBEK, D., SONNELAND, L., 2006. La Naturaleza de Los Yacimientos Naturalmente Fracturados. *Oilfield Review*.
- BREKKE, H., MACEACHERN, J.A., ROENITZ, T., DASHTGARD, S.E., 2017. The Use of Microresistivity Image Logs for Facies Interpretations: An Example in Point-Bar Deposits of The McMurray Formation, Alberta, Canada. *AAPG Bulletin*, v. 101, no.5, 655–682.

- BROUWER, F., & HUCK, A., 2011. An Integrated Workflow to Optimize Discontinuity Attributes for the Imaging of Faults. In *Attributes: New Views on Seismic Imaging—Their Use in Exploration and Production*.
- BROWN, A., 2001. Understanding Seismic Attributes. *Geophysics* V. 66. P. 46-48.
- CAINELLI, C., MOHRIAK, W.U., 1999. General Evolution of The Eastern Brazilian Continental Margin. *The Leading Edge* 18, 1–5. <https://doi.org/10.1190/1.1438387>.
- CATALDO, R., and PEREIRA E., 2018. Simultaneous Pre-Stack Seismic Inversion in a Carbonate Reservoir. Universidade Estadual de Campinas – UNICAMP, Instituto de Geociências, Campinas - São Paulo – Brasil.
- CHANG, H.K., KOWSMANN, R.O., FIGUEIREDO, A.M.F.& BENDER, A.A., 1992. Tectonics and Stratigraphy of The East Brazil Rift System (EBRIS): an overview. *Tectonophysics* 213, 97-138.
- CHANG, H. K., ASSINE, M. L., CORRÊA, F. S., TINEN, J. S., VIDAL, A. C., & KOIKE, L., 2008. Sistemas petrolíferos e modelos de acumulação de hidrocarbonetos na Bacia de Santos. *Revista Brasileira de Geociências*, v. 38, n. 2 suppl, p. 29-46.
- CHEN, Q. & SIDNEY, S., 1997. Seismic Attribute Technology Forecasting and Monitoring the Leading Edge, No. 5.
- CHOPRA, S., MARFURT, K. J., 2005. Seismic Attributes – A Historical Perspective. *Geophysics*, Vol.70; No.5.
- CHOPRA, S., & MARFURT, K., 2007. Curvature Attribute Applications to 3D Surface Seismic Data. *The Leading Edge*, 26(4), 404–414. <https://doi.org/10.1190/1.2723201>.
- CHOPRA, SATINDER Y MARFURT, KURT. J., 2007. Seismic Attributes for Prospect Identification and Reservoir Characterization. *Geophysical Developments*, No 11.

- CHOPRA, S., MARFURT, K., 2008. Gleaning Meaningful Information from Seismic Attributes. *First Break* 26, 43–53. <https://doi.org/10.3997/1365-2397.2008012>.
- CORREA R., PEREIRA C., CRUZ F., LISBOA S., JUNIOR M., CARVALHO B., SOUZA V., ROCHA C., ARAUJO F., 2019. Integrated Seismic-Log-Core-Test Fracture Characterization, Barra Velha Formation, Pre-salt of Santos Basin. Adapted from extended abstract prepared in conjunction with poster presentation given at 2019 AAPG Annual Convention and Exhibition, San Antonio, Texas, May 19-22.
- DAVISON, I., ANDERSON, L., NUTTALL, P., 2012. Salt Deposition, Loading and Gravity Drainage in the Campos and Santos Salt Basins. *Geological Society Special Publication* 363, 159–174. <https://doi.org/10.1144/SP363.8>
- DENG, X.L.; LI, J.H.; LIU, L.; REN, K.X., 2015. Advances in the Study of Fractured Reservoir Characterization and Modelling. *Geol. J. China Univ.*, 21, 306–319.
- DE OLIVEIRA, R., & DOS SANTOS, A., 2017. Bacia de Santos, Agência Nacional do Petróleo, Gás Natural e Biocombustíveis, Brasil 14ª Rodada de Licitações da ANP.
- DORN, G. A., 1998, *Modern 3D Seismic Interpretation: The Leading Edge*, v. 17, p. 1262– 1272.
- ESTRELLA, G., 2011. “Pre-Salt Production Development in Brazil”. 20th World Petroleum Congress. Head of Exploration and Production, Petrobras.
- GOMEZ, L., 2018. Estudio Petrosísmico de las Electrofacies del JSK. Tesis para Obtener el Título de Ingeniero Geofísico. Instituto Politécnico Nacional. Escuela Superior de Ingeniería y Arquitectura. Ciudad de México.
- GOMES, P.O., KILSDONK, B., MINKEN, J., GROW, T., BARRAGAN, R., 2008. The Outer High of The Santos Basin, Southern São Paulo Plateau, Brazil: Pre-Salt Exploration Outbreak, Paleogeographic Setting, and Evolution of The Syn-Rift Structures. AAPG International Conference and Exhibition, Cape Town, South Africa 10193, 26–29.

- HALLER, D. & PORTURAS, F. 1998. How to Characterize Fractures in Reservoirs Using Borehole and Core Images: Case Studies In: HARVEY, P. K. & LOVELL, M. A. (eds) *Core-Log Integration*, Geological Society, London, Special Publications, 136, 249-259.
- HEIDBACH, O., BARTH, A., MÜLLER, B., REINECKER, J., STEPHANSSON, O., TINGAY, M., ZANG, A., 2016. WSM Quality Ranking Scheme, Database Description and Analysis Guidelines for Stress Indicator. World Stress Map Technical Report 16-01, GFZ German Research Centre for Geosciences.
- HERLINGER, R., ZAMBONATO, E., and DE ROS, L., 2017. Influence of Diagenesis on the Quality of Lower Cretaceous Pre-Salt Lacustrine Carbonate Reservoirs from Northern Campos Basin, Offshore Brazil, *Journal of Sedimentary Research*, v. 87, 1285–1313.
- HUAPENG NIU, SHICHEN LIU, JIN LAI, GUIWEN WANG, BINGCHANG LIU, YUQIANG XIE, WEIBIAO XIE, 2019. In-Situ Stress Determination and Fracture Characterization Using Image Logs: The Paleogene Dongying Formation in Nanpu Sag, Bohai Bay Basin, China, *Energy Science & Engineering* published by the Society of Chemical Industry and John Wiley & Sons Ltd; 8:476–489.
- JAGLAN, H., QAYYUM, F., 2015. Unconventional Seismic Attributes for Fracture Characterization. *First Break* 33, 101–109.
- JU W., WANG K., 2018. A Preliminary Study of The Present-Day In-Situ Stress State in The Ahe Tight Gas Reservoir, Dibei Gasfield, Kuqa Depression. *Mar Pet Geol.* 2018;96:154-165.
- KATTAH, S., 2017. “Exploration Opportunities in The Pre-Salt Play, Deepwater Campos Basin, Brazil”. *SEPM, Sedimentary Record* magazine.
- KHOSHBAKHT, F., AZIZZADEH, M., MEMARIAN, H., NOUROZI, G.H., MOALLEMI, S.A. 2012. Comparison of Electrical Image Log with Core in A Fractured Carbonate Reservoir. *Journal of Petroleum Science and Engineering*, 86–87, 289–296. doi:10.1016/j.petrol.2012.03.007.

- KHOSHBAKHT, F., MEMARIAN, H., MOHAMMADNIA, M., 2009. Comparison of Asmari, Pabdeh And Gurpi Formation's Fractures, Derived from Image Log. *J Pet Sci Eng.* 2009;67:65-74.
- KINGDON, A., FELLGETT, M.W., WILLIAMS, J.D.O., 2016. Use of Borehole Imaging to Improve Understanding of The In-Situ Stress Orientation of Central and Northern England And Its Implications for Unconventional Hydrocarbon Resources. *Marine and Petroleum Geology*, 73, 1-20.
- LACOPINI, D., ALVARENGA, R., KUCHLE, J., GOLDBERG, K., and KNELLER, B., 2017. "Seismic Characterization of The Pre-Salt Rifted Section of The Lagoa Feia Group, Campos Basin, Offshore Brazil". AAPG Annual Convention and Exhibition, Houston, Texas.
- LAI, J., WANG, G., WANG, S., CAO, J., LI, M., PANG, X., HAN, C., FAN, X., YANG, L., HE, Z., QIN, Z., 2018. A Review on The Applications of Image Logs in Structural Analysis and Sedimentary Characterization. *Marine and Petroleum Geology*, 95,139-166.
- LEPLEY, S., PICCOLI, L., CHITALE, V., KELLEY, I., and QUEST, M., 2017. "The Importance of Understanding Diagenesis for The Development of Pre-Salt Lacustrine Carbonates". AAPG Annual Convention and Exhibition, Houston, Texas.
- MAERTEN, L and MAERTEN, F., 2006. Chronologic Modeling of Faulted and Fractured Reservoirs Using Geomechanically Based Restoration: Technique and Industry Applications. *AAPG Bulletin*, v. 90, no. 8, pp. 1201–1226.
- MAGNERON, C., BOURGES, M., JEANNEE, N., 2009. M-Factorial Kriging for Seismic Data Noise Attenuation 1651–1654. https://doi.org/10.3997/2214-4609-pdb.195.1904_evt_6year_2009
- MILANI, E. J., BRANDÃO, J. A. S. L., ZALÁN, P. V., & GAMBOA, L. A. P., 2000 *Petróleo Na Margem Continental Brasileira: Geologia, Exploração, Resultados E Perspectivas. Brazilian Journal of Geophysics*, vol. 18(3).

- MINZONI, M., CANTELLI, A., THORNTON, J. & WIGNALL, B., 2020. Seismic-Scale Geometries and Sequence-Stratigraphic Architecture of Early Cretaceous Syn-Post Rift Carbonate Systems, Pre-salt Section, Brazil. Published by The Geological Society of London.
- MOREIRA, J. L. P., MADEIRA, C. V., GIL, J. A., MACHADO, M. A. P., 2007. Bacia de Santos. Boletim de Geociências. Petrobras, Rio de Janeiro, v. 15, n. 2, p. 531-549, maio/nov.
- MORLEY, C. K., NELSON, R. A., PATTON, T. L. E MUNN, S. G., 1990. Transfer Zones in The East African Rift System and Their Relevance to Hydrocarbon Exploration in Rifts: AAPG Bulletin, 74:1234–1253.
- NASSERI, A., MOHAMMADZADEH, M., RAEISI, H., 2015. Fracture Enhancement Based on Artificial Ants and Fuzzy C-Means Clustering (FCMC) in Dezful Embayment of Iran. J. Geophys. Eng. 2015, 12, 227–241.
- NAURIYAL, A., SARKAR, A., KAMAT. V., 2010., Identification of Discontinuities by Attribute Analysis and Planning of Wells for Basement Exploitation – A Case Study in Mumbai High Field. 8th Biennial International Conference and Exposition on Petroleum Geophysics.
- NIAN, T., WANG, G., XIAO, C., ZHOU, L., DENG, L., LI R., 2016. The in-Situ Stress Determination from Borehole Image Logs in The Kuqa Depression. J Natural Gas Sci Eng. 2016;34:1077-1084.
- OJEDA, H.A., 1982. Structural Framework, Stratigraphy and Evolution of Brazilian Marginal Basins. American Association of Petroleum Geologists Bulletin 66, 732-749.
- OLIVEIRA, T., CRUZ, N., CRUZ, J., CUNHA, R., MATOS, M., 2019. Faults, Fractures and Karst Zones Characterization in a Pre-Salt Reservoir using Geometric Attributes 1–5.

- PEDERSEN, S.I., SKOV, T., HETLELID, A., FAYEMENDY, P., RANDEN, T., SONNELAND, L., 2003, New Paradigm of Fault Interpretation: SEG Expanded Abstracts, 350-353.
- PEREIRA, M.J., FEIJÓ, F.J., 1994. Bacia de Santos. Estratigrafia das Bacias Sedimentares do Brasil. Bol. Geociências Petrobras 8, 219–234.
- PEREIRA, M.J., MACEDO, J.M., 1990. A Bacia de Santos: Perspectivas de Uma Nova Província Petrolífera Na Plataforma Continental Sudeste Brasileira. Bol. Geociências Petrobras 4, 3–11.
- PLUMB, R.A. AND S.H. HICKMAN, 1985. Stress-Induced Borehole Enlargement: A Comparison Between the Four-Arm Dipmeter and the Borehole Televiwer in The Auburn Geothermal Well. - J. Geophys. Res., 90, 5513-5521.
- QUILEN, K., 2006. Integración de Atributos Sísmicos con Datos Petrofísicos para Determinar Zonas Prospectivas, Arena L2M, Área De Finca-Yopales. Universidad Simón Bolívar.
- RIBEIRO, S., and PEREIRA, E., 2017. Tectono-Stratigraphic Evolution of Lapa Field Pre-Salt Section, Santos Basin (Brazilian Continental Margin). Journal of Sedimentary Environments, Published by Universidade do Estado do Rio de Janeiro.
- RICCOMINI, C., SANT, L.G., TASSINARI, C.C.G., 2012. Pré-Sal: Geologia e Exploração. Revista USP (95), 33-42.
- ROBERTS, A., 2001, Curvature attributes and their application to 3D interpreted horizons. First Break, 19, 85-99.
- SCHLUMBERGER, 2009B. Petrel 2009. Seismic to Simulation Software Manual: Seismic Visualization and Interpretation Course, Houston.
- SHEN, L., SCHMITT, D.R., AND HAUG, K., 2018. Measurements of The States of In Situ Stress for The Duvernay Formation Near Fox Creek, West-Central Alberta; Alberta Energy Regulator / Alberta Geological Survey, AER/AGS Report 97, 29 p.

- SHERIFF, R., 1992. Reservoir Geophysics. Investigations in Geophysics N°7. Society of Exploration Geophysicists, Tulsa.
- SILVA, C., MARCOLINO, C., LIMA, F., SCHLUMBERGER, PETROBRAS, 2005. Automatic Fault Extraction Using Ant Tracking Algorithm in the Marlim South Field, Campos Basin. SEG/Houston 2005 Annual Meeting.
- SUN, D., LING, Y., BAI, Y., ZHANG, X., XI, X., 2011. Application of Spectral Decomposition and Ant Tracking to Fractured Carbonate Reservoirs. 73rd EAGE Conference & Exhibition incorporating SPE EUROPEC 2011 Vienna, Austria, 23-26.
- TALEBI, H., ALAVI, S.A., SHERKATI, S., GHASSEMI, M.R. AND GOLALZADEH, A., 2018. In-Situ Stress Regime in The Asmari Reservoir of The Zeloi And Lali Oil Fields, Northwest of The Dezful Embayment in Zagros Fold-Thrust Belt, Iran. GEOSCIENCES 106 53-68.
- TAENER, M., J. SCHUELKE, R. O'DOHERTY & E. BAYSAL, 2001. Seismic Attributes Revised. SEG Extended Abstract, 94, p. 1004-1006.
- VELTMAN, W., VELEZ, E., LUJAN, V., 2012. A Fresh Look for Natural Fracture Characterization Using Advance Borehole Acoustics Techniques. Adapted from extended abstract prepared in conjunction with oral presentation at AAPG Annual Convention and Exhibition, Long Beach, California, AAPG©2012.
- YILMAZ, O., 2001. Seismic Data Analysis Processing, Inversion, and Interpretation of Seismic Data (S. M. Doherty, ed.). Retrieved from <https://library.seg.org/doi/book/10.1190/1.9781560801580>.
- WRIGHT, V. P. and BARNETT, A. J., 2015. An Abiotic Model for The Development of Textures in Some South Atlantic Early Cretaceous Lacustrine Carbonates. Geological Society, London, Special Publications, v. 418, n. 1, p. 209-219.
- ZALÁN, P. V., 2004. Evolução Fanerozóica Das Bacias Sedimentares Brasileiras. Petrobras, E&P, E&P-Exp, GPE, NNE, Rio de Janeiro, RJ.

ZALÁN, P. V., OLIVEIRA, J. A. B., 2005. Origem E Evolução Estrutural Do Sistema De Riftes Cenozoicos Do Sudeste Do Brasil. Boletim de Geociências da Petrobras, Rio de Janeiro, v. 13, n. 2, p. 269-300, maio/nov.

ZHANG J., YIN S., 2019. A Three-Dimensional Solution of Hydraulic Fracture Width for Wellbore Strengthening Applications. Pet Sci. 2019;16:808-815.

Article 2: DISCRETE FRACTURE NETWORK MODELING BASED ON FRACTURE INTENSITY DERIVED FROM BOREHOLE IMAGE LOGS AND SEISMIC ATTRIBUTES BY INCORPORATING SUPERVISED NEURAL NETWORKS: THE PRE-SALT SECTION OF THE SANTOS BASIN, BRAZIL

ABSTRACT

Due to similarities in tectonic evolution, stratigraphy, and analogous petroleum systems with the prolific Campos Basin, the Santos Basin is equally considered a prolific basin with great potential for exploration of hydrocarbons. The pre-salt play is mainly comprised of lacustrine carbonates with high permeabilities. The permeability is primarily controlled by high fracture intensities and carbonate dissolution, therefore predicting the behavior of natural fractures allow to enhance the productivity of the reservoir which is highly influenced by the characteristics of the fractures in terms of intensity, orientation and spatial distribution, identified in the development of the discrete fracture network modeling. In this work, the fracture model is based on open fractures interpreted from UBI image logs which allowed the definition of four sets of fractures. Sets 1 and 2 follow a strike parallel to SHmax NE-SW and Sets 3 and 4 follow a strike parallel to Shmin; additionally, the parameters used to build the fracture model include the intensity, length, aperture, orientation, and geometry of the fractures. The fracture intensity was distributed in the geological grid according to the density of fractures per unit Area/Volume (P32) and, because fracture intensity is limited to the wellbore and its distribution is highly uncertain in regions away from the well, a supervised neural network technique was used, for which several seismic attributes such as curvature, chaos, variance, and ant tracking dedicated to the identification of faults and large fractures were generated, which were used as drivers to distribute the intensity, guided or supervised by the already known fracture intensity. Further, the ant-tracking attribute is used for estimating fracture length. The aperture is measured directly from the image logs, the orientation was based in the defined fracture sets and the geometry for the model is approximately rectangular. As the intensity of fractures is limited to the wellbore and its distribution is somewhat uncertain for regions far from the wellbore, attributes such as curvature, chaos, variance and ant-tracking were integrated as proxies for the distribution of fracture intensities. Finally, with the DFN model the fracture properties, such as permeability in three directions (I, J and K) and porosity are upscaled to a 3D geological grid based on the Oda method; through this method, it was possible to infer a permeability behavior

expressed by $K_j > K_i > K_k$, highlighting that the K_j direction contains the best permeability responses, and further suggesting a good connectivity for the fractures of the main structural systems F1 and F2 parallel to the SHmax direction. Outputs from this work can be used to construct geomechanical reservoir models that allow a better understanding of matrix-fracture relationships.

INTRODUCTION

Recent studies have revealed that the Santos Basin can be considered a prolific basin of vast potential for hydrocarbon exploration, this due in large part to the strong similarity with the prolific Campos Basin, which has similar tectonic evolution, stratigraphy, and petroleum systems. (Pereira and Macedo, 1990; Mello et al., 2002). Moreover, the large oil discoveries by Petrobras in Santos Basin have opened new horizons for oil exploration in the pre-salt section, located at depths greater than 6,500m just below a thick layer of evaporites in ultra-deep waters depths greater than 2,500m. The estimated reserves for this pre-salt section represent an important hydrocarbon potential and a new exploration frontier. (Chang et al., 2008).

The Santos Basin consists of a sequence of Barremian to Aptian lacustrine carbonates with high permeabilities expressed in excellent reservoir productivity. The permeability of these carbonates is primarily controlled by high fracture intensities and carbonate dissolution (e.g., karstification) (Correa et al., 2019; De Jesus et al., 2016; Duarte et al., 2018). Because discontinuities such as faults and fractures can play a critical role in creating regions with high reservoir porosity and permeability, they must be considered for reservoir modeling (Meldahl et al., 2001; Ligtenberg 2005). The incorporation of fractures into reservoir models not only reduce the geological uncertainty for exploration, but also improve the forecast of production and guide the development plans (Correa et al., 2019).

The production and development of a naturally fractured reservoir is highly influenced by the characteristics of the fracture network which may control the flow direction and volume of the hydrocarbons through the layers (Valentini et al., 2007). Having a robust knowledge of fracture characteristics in terms of intensity, orientation, and spatial distribution allows the prediction of preferential flow paths (Meldahl et al., 2001; Ligtenberg 2005), therefore, it is possible that the fracture networks are controlling the distribution of the petrophysical properties (Correia et

al., 2017). Thus, commonly discrete geological models considering the fractures (DFN – Discrete Fracture Networks) are built to understand the relationship between the networks, the porosity and permeability of the reservoir (Bourbiaux et al., 2002).

Hence, the major purpose of this research is to create a DFN model based on the distribution of fractures in a geological grid in the pre-salt reservoir of the Santos Basin, Brazil. This distribution was created by the integration of image log, seismic attribute analysis, and supervised neural networks, which are the main techniques for fracture mapping (Deng et al., 2015; Huapeng Niu et al., 2019). Furthermore, the DFN model can be used to create a geomechanical model that provides information on the regions with high porosity, permeability, and high-density of fracturing of the reservoir.

GEOLOGICAL SETTING

The Santos Basin is located in offshore southeastern Brazil (Figure 1); its tectonic evolution is associated to the rupture processes between west Africa and South America during the late Jurassic and early Cretaceous (Cainelli and Mohriak, 1999; Milani et al., 2000; Zalán, 2004), resulting in a tectonic framework consisting of horsts and grabens associated with a faulting regime with normal component and transfer faults (Ojeda, 1982; Chang et al., 1992; Gomes et al., 2008).

The study interval focuses on the pre-salt play that corresponds to the rift and post-rift super-sequences derived from the tectonostratigraphic evolution of the Santos Basin; each of these sequences is bounded by regional unconformities and the sedimentary record begins in the Hauterivian and extends up to the Aptian (Pereira y Macedo, 1990; Pereira y Feijó, 1994; Moreira et al., 2007; Davison et al., 2012) (Figure 2).

The economic basement of basin is represented by Camboriu Formation, a sequence of basalts that were deposited during the initial stage of Gondwana breakup. The lower part of syn-rift deposits corresponds to Piçarras Formation and comprise conglomerates and sandstones in the proximal portions, and lacustrine siltstones and shales in the distal portion; the upper part corresponds to the Itapema Formation dominated by organic-rich carbonates, recognized by the abundant presence of rudstones and grainstones of bivalves interbed with sandstones and

laminated mudrocks (Moreira et al., 2007). The post-rift phase includes the Barra Velha Formation, it is composed mainly of limestone, shales, and magnesium-rich claystones associated with in situ carbonates, formed in a hyperalkaline continental-marine transitional system (Moreira et al., 2007). Finally, the upper part of the post-rift phase corresponds to the evaporitic deposits of the Ariri Formation which acts as a regional seal (Moreira et al., 2007; Amaral et al., 2015).

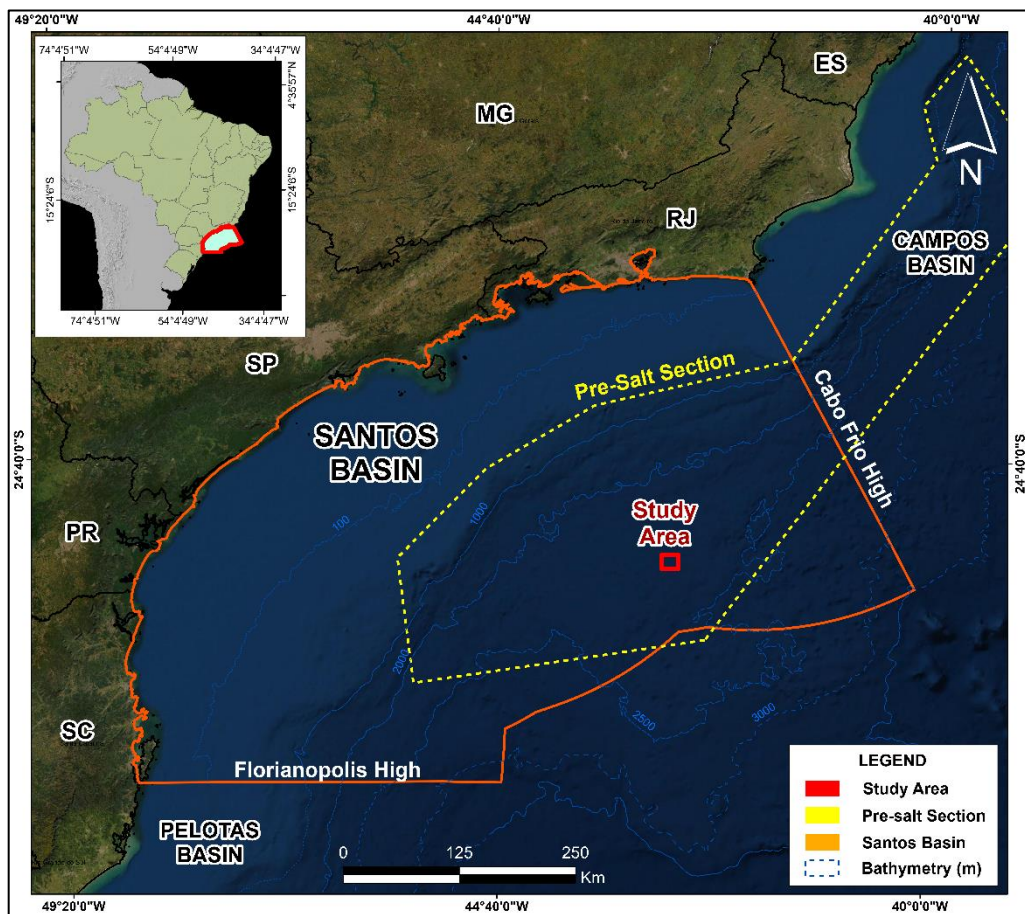


Figure 19. Location map of the study area and the Brazilian pre-salt section, situated in the SE offshore continental margin of the Santos basins. (Shapefiles taken from the Brazilian National Agency for Petroleum, Natural Gas and Biofuels, ANP).

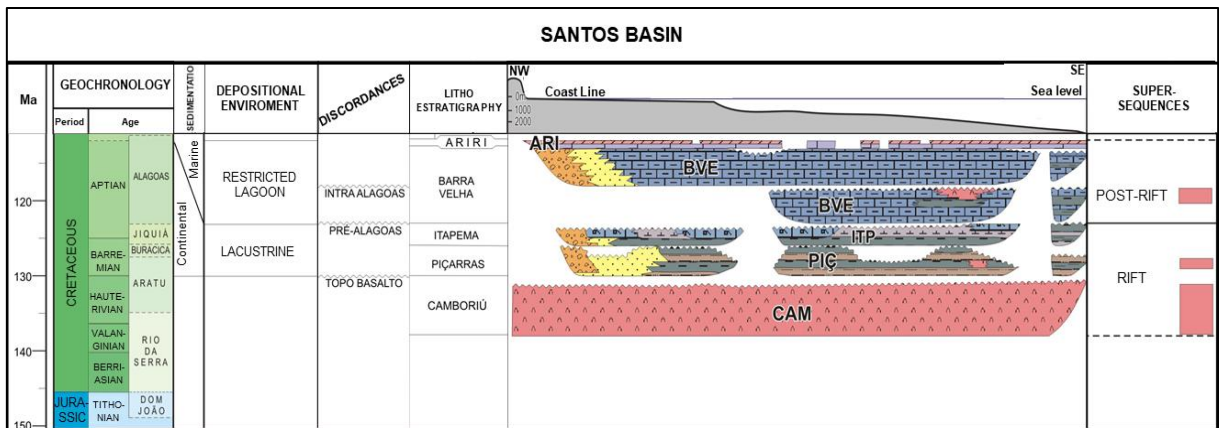


Figure 20. Lithostratigraphic chart of the rift and post-rift super-sequences of the Santos Basin. (Extracted from Moreira et al., 2007).

DATABASE AND METHODS

The input data for the DFN model was generated from four wells and includes check-shots (time-depth model), formation tops, sonic logs, density logs, and borehole image with interpretation of fracture point data such as dip angle, dip azimuth and fracture type (natural vs induced). In addition, we used a 3-D post-stack time migrated seismic survey covering an approximate area of 300 km². The seismic volume contains 650 inlines and 700 crosslines with an interval spacing of 12.5x12.5 m, and the recording interval was 8000 ms with a sampling rate of 4 milliseconds. To creating the inputs, the seismic volume was preconditioned, which involved noise removal by applying filters to eliminate seismic anomalies such as acquisition footprints or multiples in order to improve the signal-to-noise ratio and therefore the reflector continuity.

The seismic data conditioning was based on the evaluation of data mostly through amplitude maps and amplitude spectra. In this step the Dip Steered Median Filter (DSMF) is used, which changes the diffuse terminations of the reflectors closer to the fault zones with a pre-computed geometry feature, which recognizes the dissimilar seismic traces and improves the reflectors' edge (Jaglan and Qayyum, 2015).

Interpretation of fractures in image logs

The input for the fracture model relied on the interpreted open fractures of the acoustic borehole image logs. For all wells, Ultrasonic Borehole Imager tool (UBI – Schlumberger) were available for structural interpretation. The UBI tool's produces high-resolution images that

covers 360° of borehole wall and is operable in heavy water and oil-based muds (Schlumberger, 2002). The dataset was loaded and processed in Interactive Petrophysics software. The main processing involves the adjust of accelerometer acquisition and the influence of magnetic field (inclination and declination), thus it was possible to obtain the true dip and azimuth of interpreted faults and fractures on borehole images. Three structural features were interpreted in this study: Natural fractures, breakouts and drilling induced fractures. The fractures were mapped according to their sharp and continuous edges in borehole images, showing distinct dip and azimuth from sedimentary bedding planes. In vertical wells, the Breakouts and drilling induce fractures are shown as vertical structures resulting from maximum and minimum horizontal stress of the field. The breakouts are represented by continuous dark zones where the borehole wall was collapsed following the minimum horizontal stress while the drilling induced fractures occurs at vertical orientation following the maximum horizontal stress of the field (Figure 21).

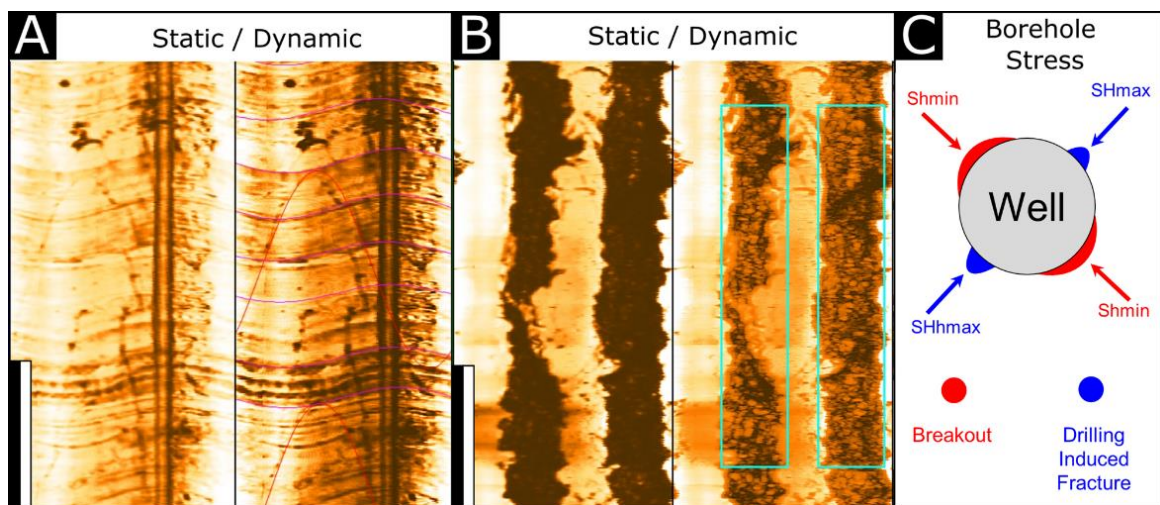


Figure 21. Acoustic image logs. A) Occurrences of natural fracture. B) Breakouts highlighted in green area. C) Representative breakout and drilling-induced fractures. The SHmax is approximately perpendicular to the breakouts, and parallel to drilling-induced fractures.

Fracture Modeling (Discrete Fracture Network – DFN)

The input for the fracture model relied on the interpreted open fractures of the UBI image logs, from which sets were defined with the structural analysis in rosettes and pole diagrams.

The main parameters for constructing the fracture model comprise the Intensity, Length, Aperture, Orientation, and Geometry of the fractures (for the model are approximated as

rectangular). The fracture intensity is the most important input to distribute the fracture in the DFN, this is because it describes the density of fractures per unit length/area/volume, therefore the intensity is the count of intersected fractures per length in 1-dimension 1D (P10), per area in 2-dimensions 2D (P22) or per volume in three-dimensions 3D (P32) (Dershowitz and Herda, 1992); thus, the fractures were distributed into the geological grid by Area/Volume (P32).

Fracture length is a difficult parameter to obtain. Although for this model, the seismic attribute ant-tracking was used, to estimate an approximate value of fracture length. The average length was 600 meters. In addition, sensitivity tests were carried out with slightly higher and lower values than the estimated by the attribute ant-tracking.

According to sensitivity tests, it was observed that the aperture is a parameter that has a high influence on the model, however it has the advantage that it can be measured in the image logs. From direct measurements, the resultant range is from 0,3 to 0,5 millimeters (mm), therefore this was the value used for the model.

Supervised Artificial Neural Networks for DFN

Artificial neural networks, which are built by artificial neurons coupled to one another to convey signals through machine learning, are computer models based on the activity seen in the human brain. Each neuron is linked to the others by connections that involve weighted processing that transforms input data subjecting it to different operations to learn and generate other output data (Jafari et al., 2012).

In this studio a supervised neural network technique was used to improve the fracture intensity (P32) distribution in the 3D grid, this is because the fracture intensity is limited to the wellbore and its distribution is highly uncertain for the regions away from the well (Figure 22). Therefore, several seismic attributes such as curvature, chaos, variance, and ant-tracking dedicated to the identification of fault and large fractures were generated to be used as inputs to distribute the fracture intensity, guided or supervised by previously obtained fracture intensity from acoustic borehole image logs. To be aware of, the settings of the neural network algorithm were set at 150 for a maximum number of interactions, 10% for error limit, and 50% for cross-validation. These parameters were utilized to keep the process error rate within

acceptable bounds and avoid overtraining according to the architecture (Figure 23). Finally, the neural net fracture intensity was used to generate the DFN model.

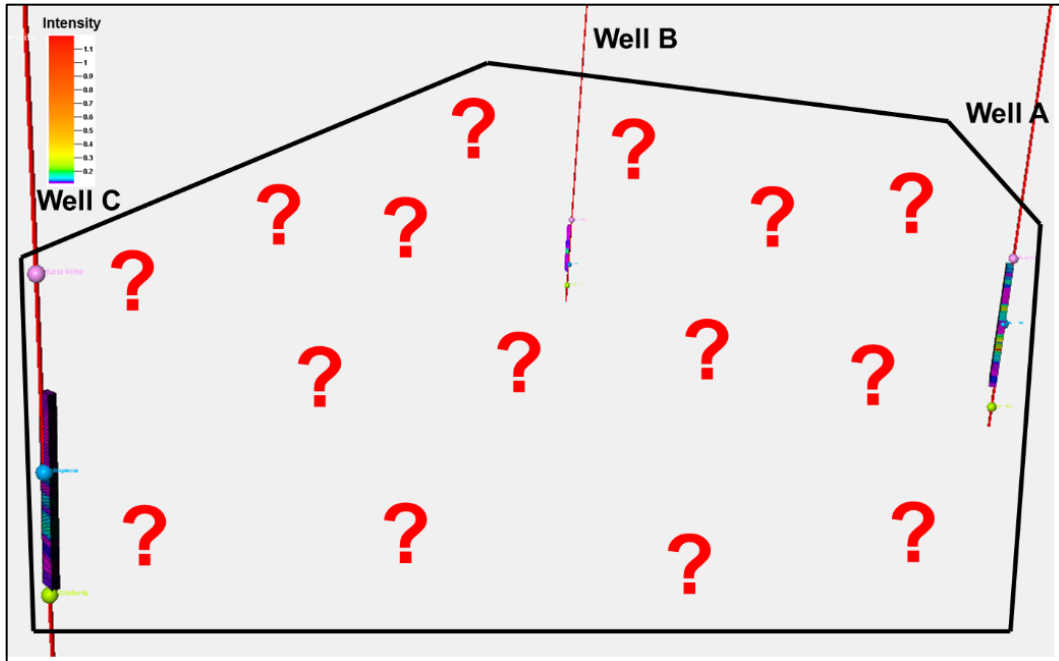


Figure 22. Schematic example: zones without information to obtain a good distribution of the fracture intensity. The fracture intensity is limited to the wellbore and its distribution is highly uncertain for the regions away from the well.

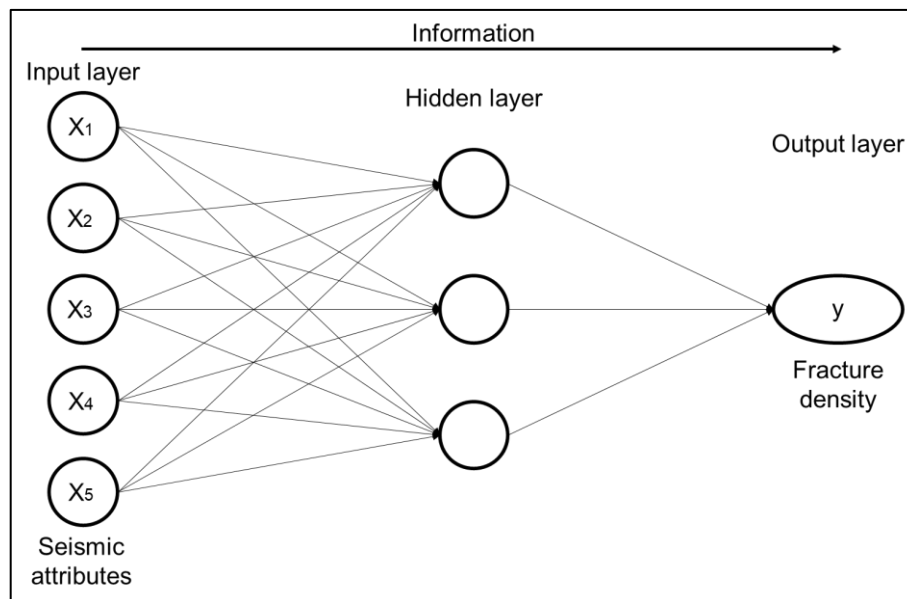


Figure 23. Global system of neural network processing used in this study.

Model Upscaling

With the previously generated fracture model, the fracture properties such as permeability in three directions (I, J, and K) and porosity are upscaled to a geological 3D grid generated from the seismic interpretation (Horizons and Faults). The upscaling was based on the Oda method (Oda, 1985); According to Derhowitz (2007), the Oda method is a fast-upscaling statistical method that estimates properties based on the total area of discrete fractures in each cell since these properties depend on the intensity, interconnectivity, and transmissivity of the fractures. In addition, it performs a numerical integration for the implicit fractures.

RESULTS AND DISCUSSION

Fracture Modeling (Discrete Fracture Network – DFN)

From the interpreted open fractures of the UBI image logs and the structural analysis in rosettes and pole diagrams, four sets of fractures were defined, the resultant fracture sets have the following preferential orientations: Sets 1 and 2 (F1 and F2 follow a strike parallel to SHmax NE-SW with average dip of 45° and 37° respectively), and Sets 3 and 4 (F3 and F4 follow a strike orthogonal to SHmax NW-SE with average dip of 53° and 43° respectively) (Figure 24).

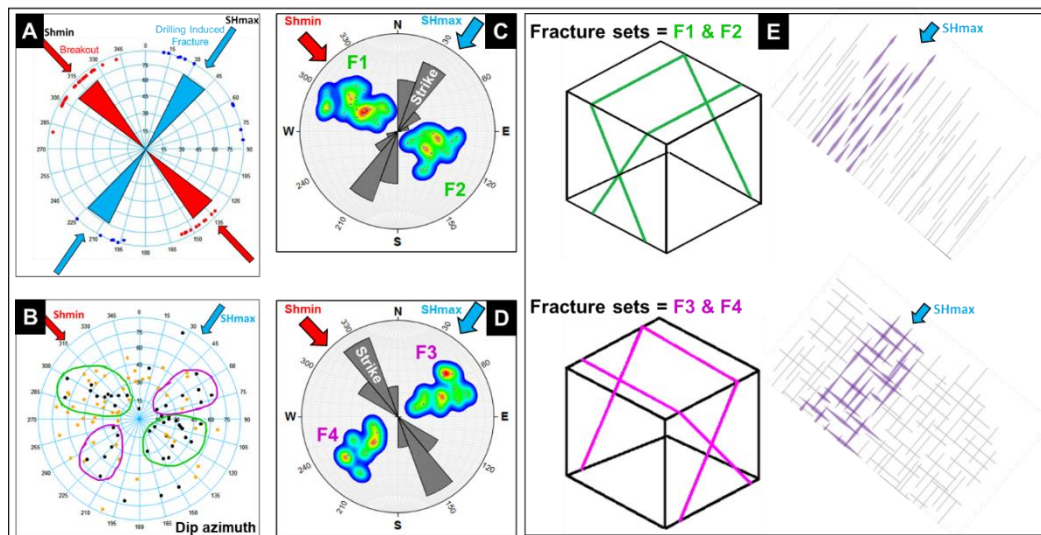


Figure 24. Summary plot of the main fracture sets identified in the pre-salt play from borehole image logs. A) The borehole breakout and drilling-induced fractures determined the orientation of the minimum horizontal stress (Shmin) and maximum horizontal stress (SHmax). B) Four fracture sets in pre-salt play are illustrated. The Dip azimuth is represented by a stereo net diagram. C) Illustrating the two main sets with a strike NE-SW parallel to SHmax. D) Illustrating the two sets with a lower prevalence with a strike NW-SE orthogonal to SHmax. E) Representative plot of the fracture sets identified in the pre-salt play from borehole image logs.

According to the available computational capacity, a geological model was defined from the interpreted horizons (Barra Velha and Camboriu formations tops) and regional faults in the pre-salt play (Figure 25). The grid was built based on the structural framework (SF) algorithm, it is defined by 322x347x385 cells spaced by a horizontal increment of approximately 50x50 m and a vertical increment of 2.5 m, resulting in a grid with approximately 43 million-cell (Figure 26). Based on the SGS algorithm (Sequential Gaussian simulation), the geological grid was statistically populated with properties, such as the fracture intensity (P32). (Figure 27).

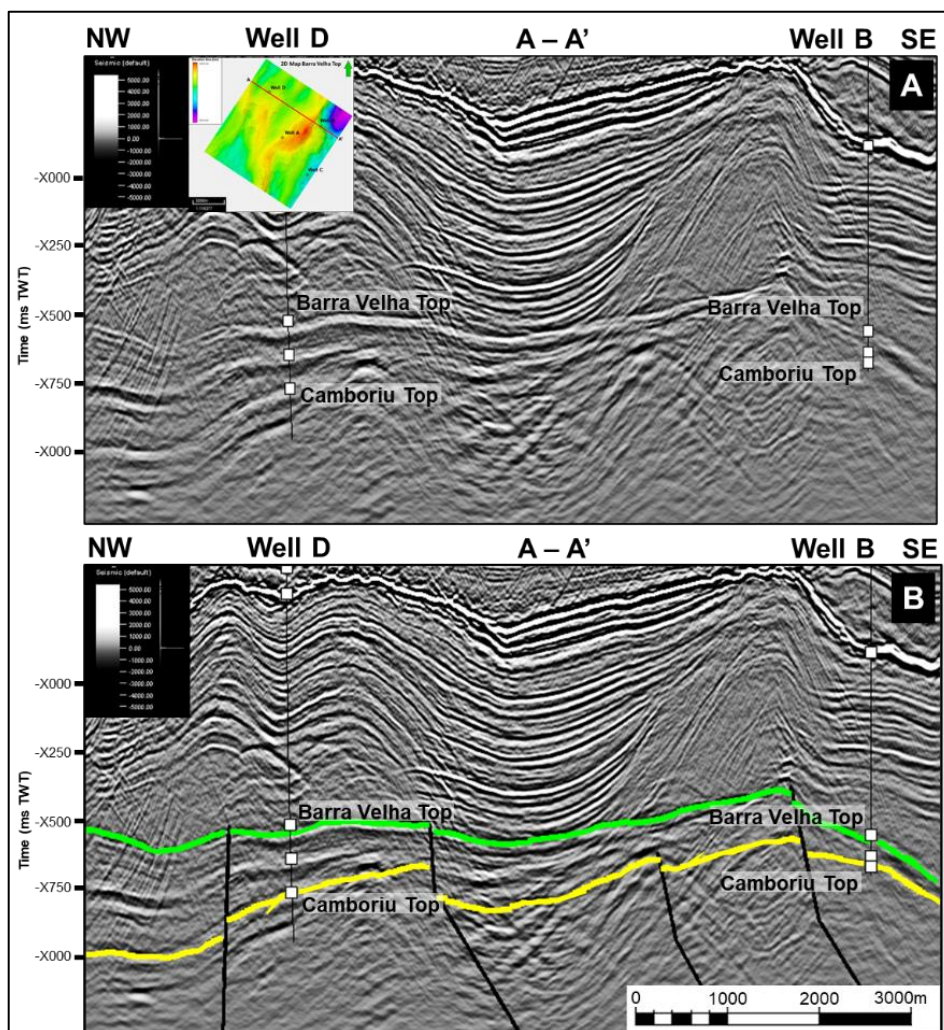


Figure 25. A) Seismic cross section (A-A') before interpretation. B) Interpreted seismic section (A-A') of the main horizons (top and base of the pre-salt play, green and yellow lines respectively) and regional faults (black lines).

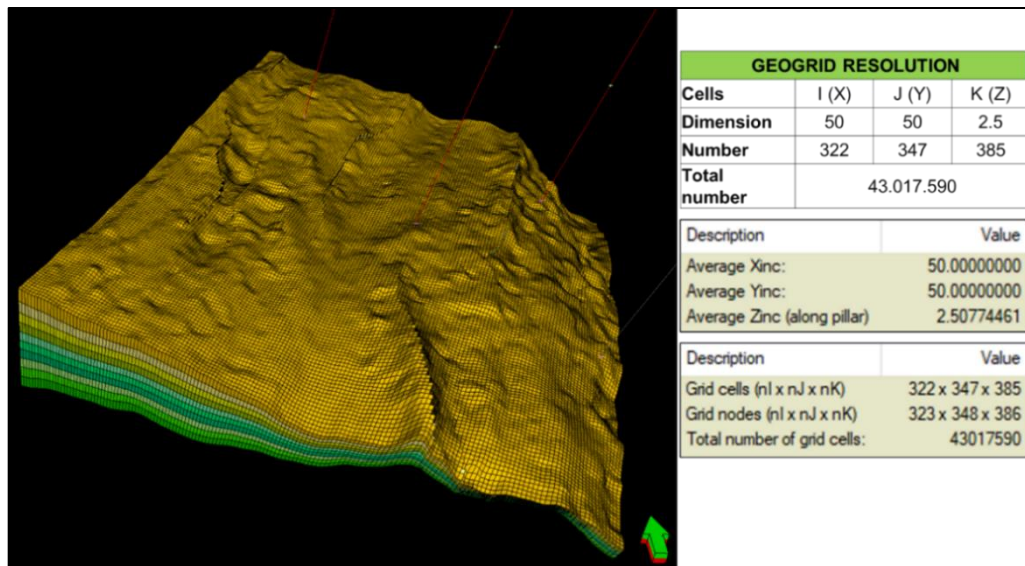


Figure 26. 3D geological grid highlighting its dimensions for upscaling fracture properties.

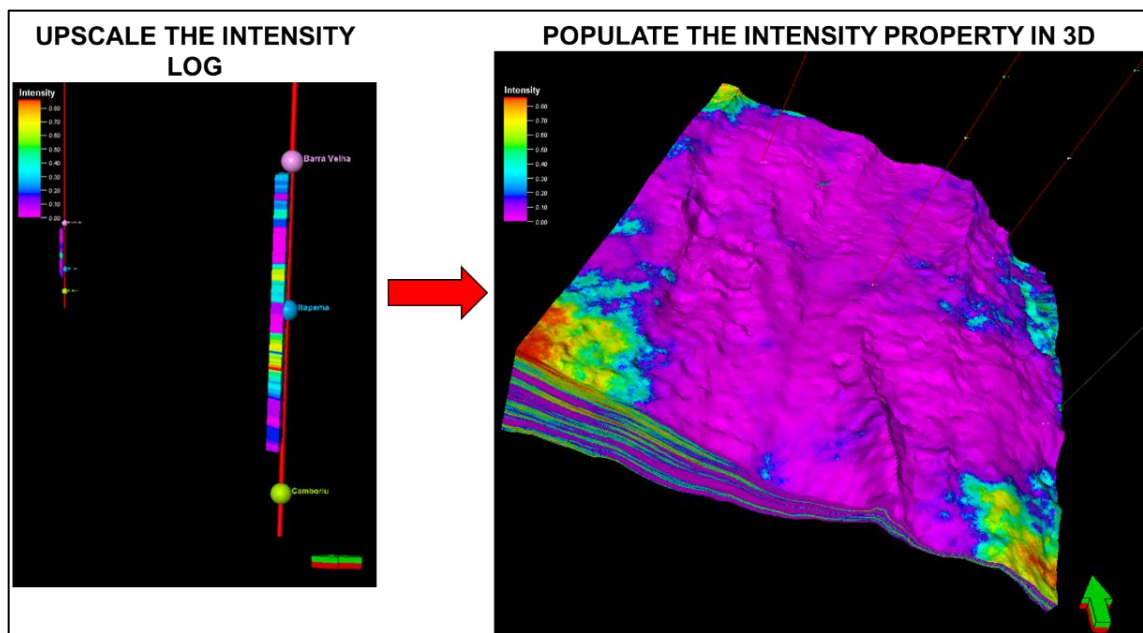


Figure 27. The upscaled fracture Intensity property is populated throughout the 3D grid.

Table 2 and Figure 28 summarize the permeability results (unscaled) obtained for each test varying the apertures of the fractures. Overall, it is observed that the fracture aperture is the property that has greatest impact on the permeability. Variations in aperture include the range of values measured in the image logs which vary between 0,3 to 0,5 mm, with values close to 0.3 occurring primarily in NW-SE strike fractures and apertures close to 0.5 occurring in NE-SW strike fractures. When comparing the results of the models with 0,3 and 0,5 mm, a large difference in permeability is observed; therefore, to have a better control in the aperture of the

fractures, the stress configuration of the pre-salt play in the study area was taken as a criterion, this assuming that the sets F1 and F2 that follow a strike parallel to SHmax NE-SW will have higher apertures (0,5 mm), whereas the sets F3 and F4 that follow a strike parallel to Shmin NW-SE will have lower values (0,3 mm) (Figure 24), correlating with what was stated by Correia et al., 2019, where assumes: "every fracture set in the direction of the SHmax would have greater aperture values, whereas fractures set in the direction of the Shmin would have lower aperture values", and with Huapeng Niu et al., 2019, in Dongying Formation of the Bohay Bay Basin of China.

Table 2. Summary of permeability results (unscaled) obtained for each test varying the apertures of the fractures (0,5 mm, 0,4 mm and 0,3 mm).

DFN MODEL	PERMEABILITY mD		
	Min	Max	Mean
Test - apertures of fracture 0,5 (mm)	163656,2	276823,7	208506,7
Test - apertures of fracture 0,4 (mm)	98582,6	190152,9	133509,9
Test - apertures of fracture 0,3 (mm)	50117,2	120305,8	75179,7

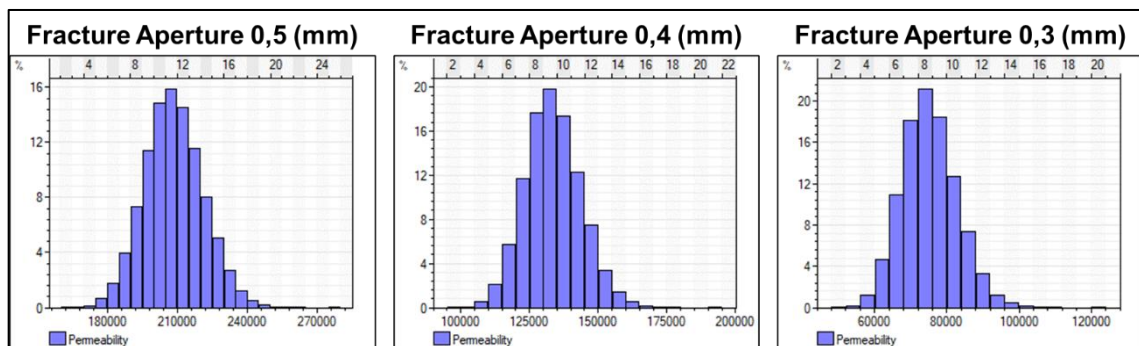


Figure 28. Permeability distribution (unscaled) obtained for each test varying the apertures of the fractures (0,5 mm, 0,4 mm and 0,3 mm).

Supervised Artificial Neural Networks for DFN

As stated in the methodology, the fracture intensity (P32) is limited to the wellbore and its distribution is highly uncertain for the regions away from the well, therefore the attributes such as curvature, chaos, variance, and ant-tracking were generated, considering that are algorithms dedicated to highlight fault and large fractures zones (Figure 29B), therefore they were considered as a second property to distribute the fractures. The correlation analysis between the different attributes according to the Figure 29A emphasizes that the ant-tracking attribute best shows the correspondence with fracture intensity. However, for the supervised neural network

all the attributes were preserved to explore relationships between the multiple parameters of each one, integrating a significant amount of information to have a more complete result and not losing important evidence of fractures. Finally, a distributed fracture intensity is obtained with the attributes derived from the seismic.

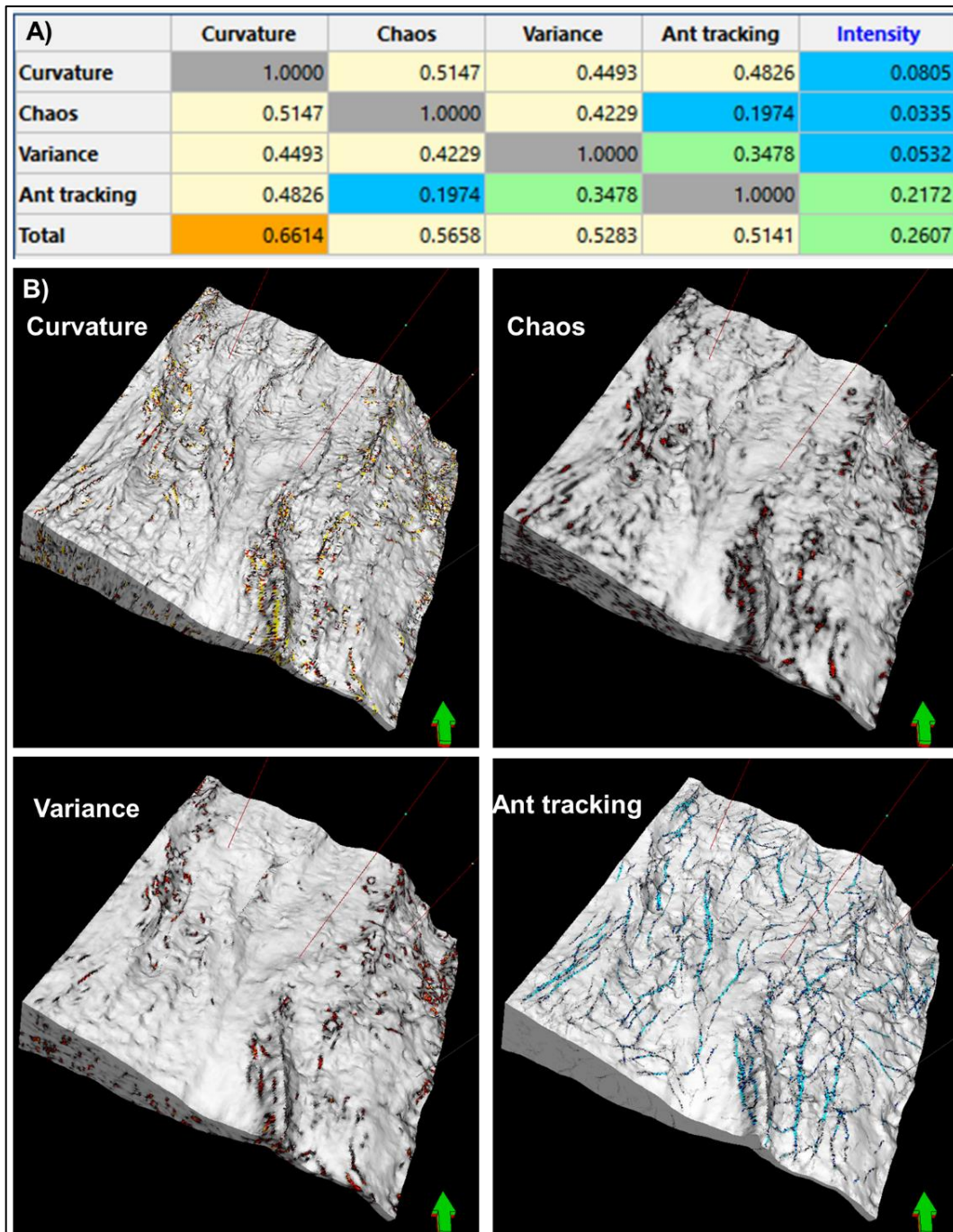


Figure 29. A) Results of the correlation analysis between the seismic attributes selected as input data for training in the supervised technique. B) Seismic attributes selected considering that are algorithms dedicated to highlight fault and large fractures zones.

The correlation coefficients between the intensity of fractures and the seismic attributes have questionable values, this may partly be due to the scarcity of well data in some areas of the study area and secondarily due to the low quality of the seismic volume. Despite that, it can be observed a good distribution of the fractures, for which the DFN model of this analysis was used to distribute the porosity and permeability of the fractures throughout the previously built 3D grid. Further, it should be noted that the results of these properties developed from the DFN must be calibrated with well tests.

Figure 30 shows the stochastic DFN model built using the Fracture Intensity derived from the supervised neural network and it is based on input thresholds of the previously calculated length, aperture, geometry and orientation parameters. Figure 31 represents the main structural systems of orientation NE-SW (Sets 1 and 2), and the lower order systems corresponding to the NW-SE orientation (Sets 3 and 4).

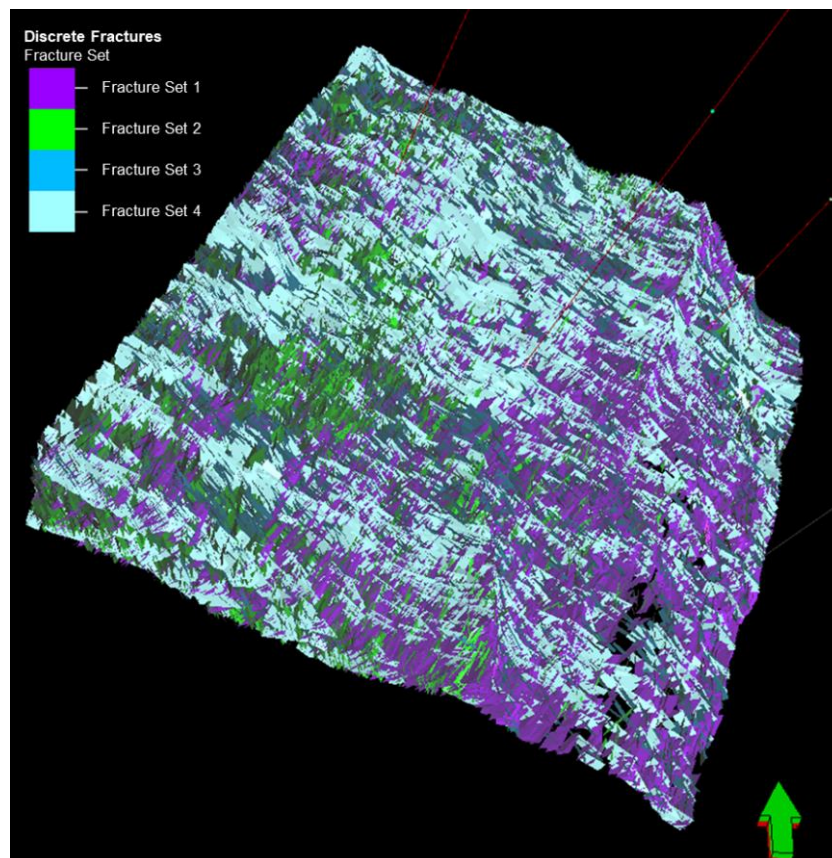


Figure 30. Stochastic DFN model built using the Fracture Intensity derived from the supervised neural network and the orientation interval for four fracture sets.

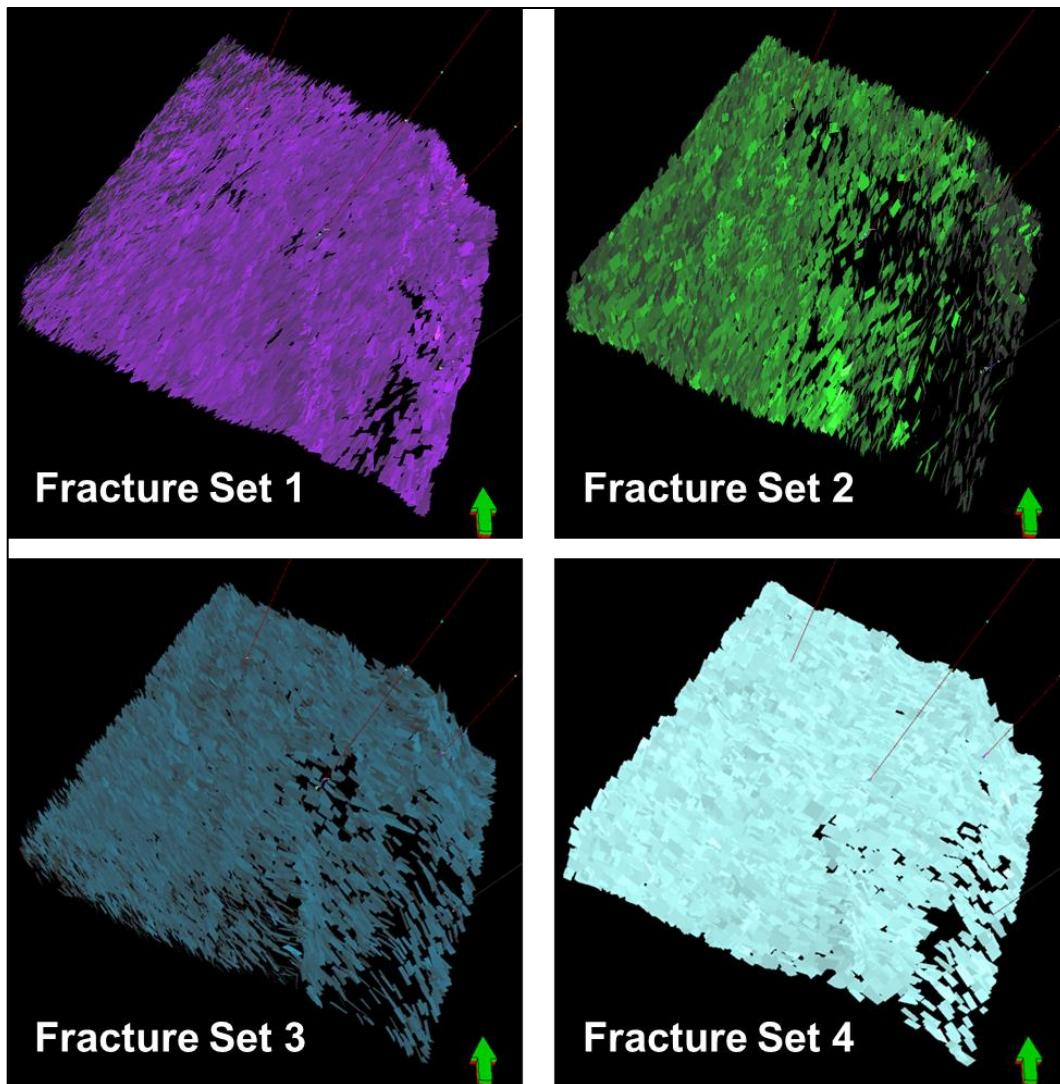


Figure 31. DFN fracture models for each fracture sets: Set 1 and 2 follow a strike NE-SW with average dip of 45° and 37° respectively; Set 3 and 4 follow a strike NW-SE with average dip of 53° and 43° respectively.

Model Upscaling

The DFN model built in the pre-salt play based on the four identified fracture sets is upscaled to the 3D grid using the Oda method discussed previously in the methodology, from which the following properties were obtained: permeability (I, J, and K directions) and porosity. The contribution of the fracture porosity in the pre-salt play is close to 0.01% and the permeability is in the range from 1,3 to 9,5 mD for direction i, 2,0 to 13,8 mD for direction j and 1,0 to 4,7 mD for direction K (Figure 32). Results according to the fracture aperture of 0,5 mm for the main structural system of NE-SW orientation (F1 and F2) and 0,3 mm for the lower order system corresponding to the NW-SE orientation (F3 and F4).

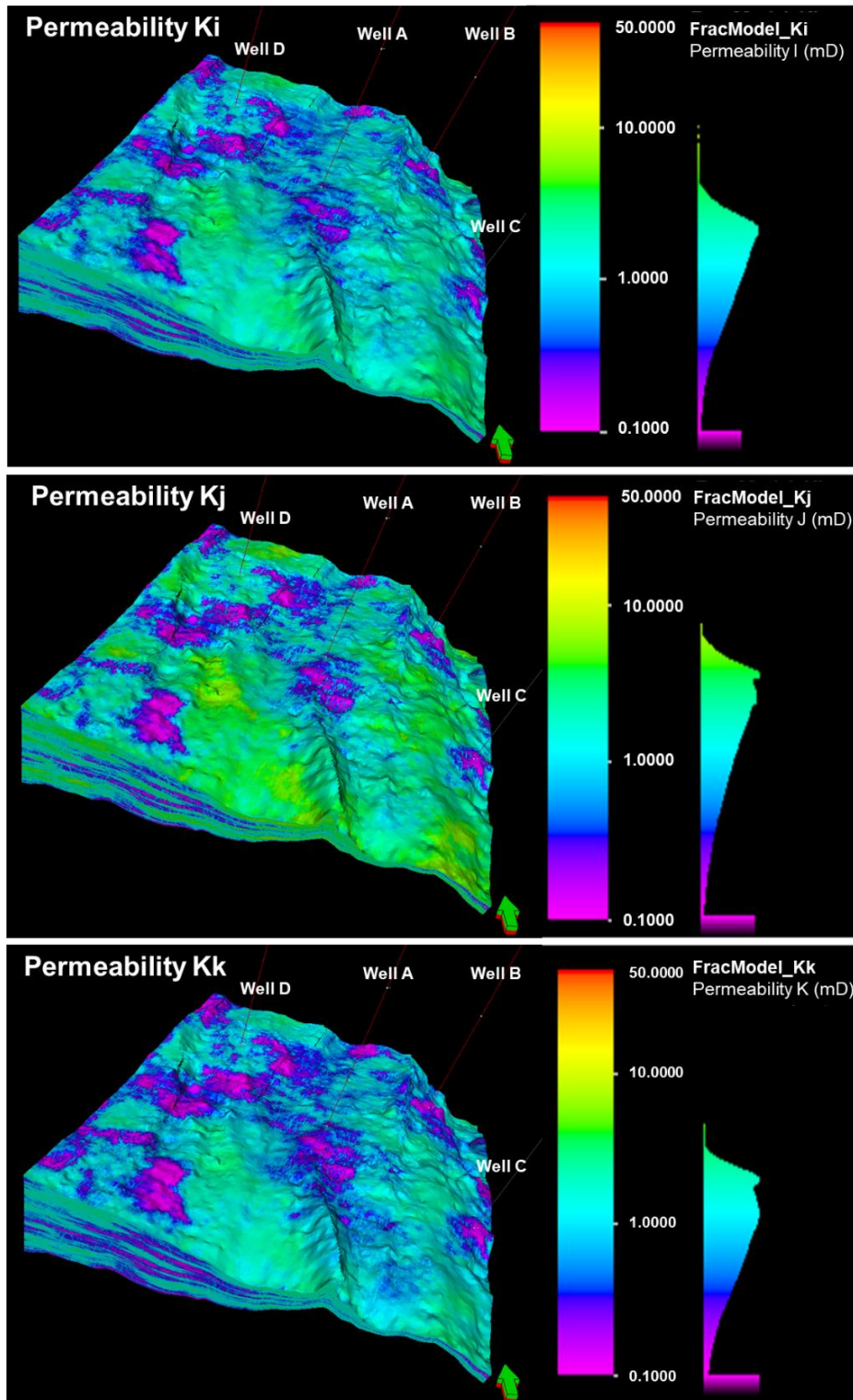


Figure 32. Fracture permeability (I, J, and K directions) for the grid DFN.

Wrapping up the understanding of the fractures in the pre-salt play with the results of the upscaled DFN model, it was possible to infer some behavior patterns of permeability that are

mainly developed with the orientation and structural position of the fractures within the paleotopographic highs of the study area, this is presented as follows:

Horizontal permeability results indicate that the K_j direction contains the highest permeabilities with values up to 13,8 mD, suggesting that in general terms the behavior of the study area is $K_j > K_i$. This indicates that the abundance of fractures of the main structural systems F1 and F2 (strike NE/SW) correspond to the higher permeabilities throughout the field. In addition, this is associated with the SH_{max} direction and the regional configuration of the study area, suggesting good connectivity for these fractures (Figure 33). Our results from the Santos Basin shows good correlation with observations from the Dongying Formation of the Bohay Bay Basin of China (Huapeng Niu et al., 2019), where fractures parallel to SH_{max} exhibit the open state and the highest connectivity between each other (see article 1).

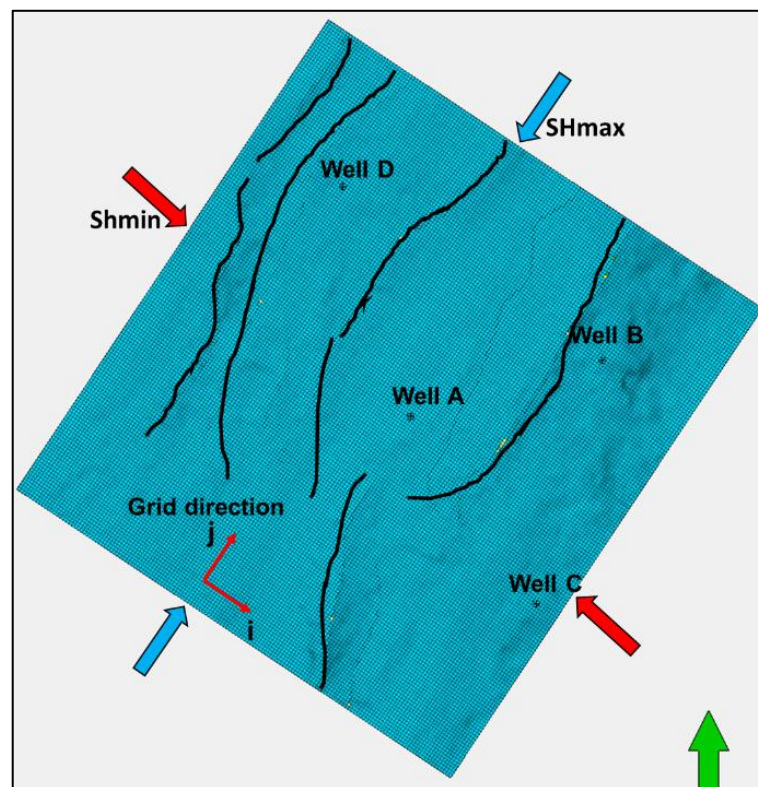


Figure 33. 2D view showing the grid direction (K_i and K_j) and the demonstration of the structural configuration of the study area.

In addition, the results of the high intensity of fractures in the direction of the maximum horizontal stress and in the paleotopographic highs suggest these zones of structural highs as

zones of interest for hydrocarbon accumulations, this due to their possible good permeability and fracture connectivity (Figure 34).

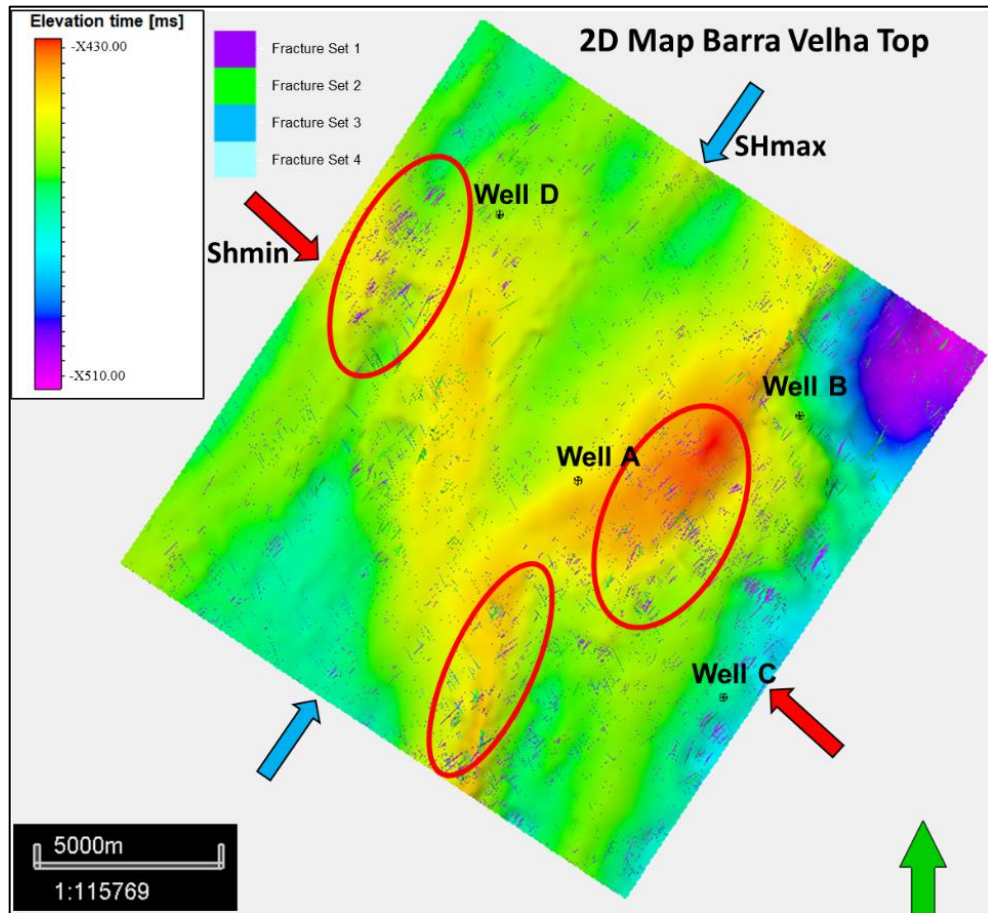


Figure 34. Three fracture zones (red circles) belonging to Sets 1 and 2, highlighting the large number of fractures in the "Kj" direction and corresponding to the structural highs, suggesting areas with possible good permeability and fracture connectivity.

CONCLUSIONS

Regarding the methodology, the main tool to build the DFN model is derived from information of UBI image logs; however, information from other sources such as seismic attributes (curvature, chaos, variance, and ant-tracking) was important to correlate and define parameters of the DFN, as well as to improve the distribution of the intensity of fractures in the 3D grid.

According to the performed study, it was possible to observe that the determining parameters of the permeability of the fractures based on the DFN are the Intensity, Length, Aperture, Orientation, and Geometry of the fractures. Of all these parameters, the aperture has the greatest

influence in the permeability, therefore for our analysis we measure the aperture of the fractures in the image logs and assume that the sets with a strike parallel to SHmax will have higher apertures and the sets that follow a strike parallel to Shmin will have lower values. In addition, it was observed that the fracture length parameter is a property that does not greatly impact the results, this possibly because the spaces not occupied by large fractures would be occupied by shorter ones.

With the results of the upscaled DFN model, it was possible to find or infer a behavior of the patterns of permeability, developed with the following configuration $K_j > K_i > K_k$. According to the horizontal permeability, the K_j direction contains the highest permeability responses, thus suggesting good connectivity for the fractures belonging to the main structural systems F1 and F2 associated with the SHmax direction and the regional tectonic configuration of the study area.

Outputs and observations from this work can be used to create geomechanical earth models, which will further allow a better understanding of matrix-fracture relationships.

REFERENCES

- ABDIDEH, M., and AMANIPOOR, H., 2012. Fractures and Borehole Breakouts Analysis of a Reservoir Using an Image Log (Case Study: SW Iran). *Petroleum Science and Technology*, 30:22, 2360-2372. DOI: 10.1080/10916466.2010.512895.
- AGUILERA, R. 1995. Naturally Fractured Reservoir. Second edition. Tulsa, Oklahoma: PennWell Publishing Company. ISBN 0-87814-449-8
- AMARAL, P. J., MAUL, A. R., FALCÃO, L., CRUZ, N. M., GONZALEZ, M. A., & GONZÁLEZ, G., 2015. Estudo Estatístico da Velocidade Dos Sais Na Camada Evaporítica Na Bacia De Santos. 14th International Congress of the Brazilian Geophysical Society & EXPOGEF, Rio de Janeiro, Brazil, 3-6 August 2015. Brazilian Geophysical Society. p. 666-669.
- ARIZA, D., MOREIRA, W., DE ANDRADE, I., RODRIGUES, J., FERRARI, A., PIERANTONI, L. AND OLHO, M., 2019. Unsupervised Seismic Facies

Classification Applied to a Pre-Salt Carbonate Reservoir, Santos Basin, Offshore Brazil. AAPG Bulletin, v. 103, no. 4 (April 2019), pp. 997–1012.

BAHORICH, M.S., and FARMER, S.L., 1995, 3-D Seismic Discontinuity for Faults and Stratigraphic Features: The Coherence Cube: SEG Expanded Abstract, 93-96.

BOURBIAUX, B., BASQUET, R., CACAS, M.C., DANIEL, J.M., SARDA, S., 2002. An integrated workflow to account for multi-scale fractures in reservoir simulation models: implementation and benefits. In Abu Dhabi International Petroleum Exhibition and Conference. Society of Petroleum Engineers, <https://doi.org/10.2118/78489-MS>.

BRATTON, T., VIET CANH, D., VAN QUE, N., DUC, N., GILLESPIE, P., HUNT, D., LI, B., MARCINEW, R., RAY, S., MONTARON, B., NELSON, R., SCHODERBEK, D., SONNELAND, L., 2006. La Naturaleza de Los Yacimientos Naturalmente Fracturados. Oilfield Review.

BROUWER, F., & HUCK, A., 2011. An Integrated Workflow to Optimize Discontinuity Attributes for the Imaging of Faults. In Attributes: New Views on Seismic Imaging—Their Use in Exploration and Production.

BROWN, A., 2001. Understanding Seismic Attributes. Geophysics V. 66. P. 46-48.

CAINELLI, C., MOHRIAK, W.U., 1999. General Evolution of The Eastern Brazilian Continental Margin. The Leading Edge 18, 1–5. <https://doi.org/10.1190/1.1438387>.

CHANG, H. K., ASSINE, M. L., CORRÊA, F. S., TINEN, J. S., VIDAL, A. C., & KOIKE, L., 2008. Sistemas petrolíferos e modelos de acumulação de hidrocarbonetos na Bacia de Santos. Revista Brasileira de Geociências, v. 38, n. 2 suppl, p. 29-46.

CHANG, H.K., KOWSMANN, R.O., FIGUEIREDO, A.M.F.& BENDER, A.A., 1992. Tectonics and Stratigraphy of The East Brazil Rift System (EBRIS): an overview. Tectonophysics 213, 97-138.

- CHEN, Q. & SIDNEY, S., 1997. Seismic Attribute Technology Forecasting and Monitoring the Leading Edge, No. 5.
- CHOPRA, S., MARFURT, K. J., 2005. Seismic Attributes – A Historical Perspective. *Geophysics*, Vol.70; No.5.
- CHOPRA, S., & MARFURT, K., 2007. Curvature Attribute Applications to 3D Surface Seismic Data. *The Leading Edge*, 26(4), 404–414. <https://doi.org/10.1190/1.2723201>
- CHOPRA, SATINDER Y MARFURT, KURT. J., 2007. Seismic Attributes for Prospect Identification and Reservoir Characterization. *Geophysical Developments*, No 11.
- CHOPRA, S., MARFURT, K., 2008. Gleaning Meaningful Information from Seismic Attributes. *First Break* 26, 43–53. <https://doi.org/10.3997/1365-2397.2008012>.
- CORREA R., PEREIRA C., CRUZ F., LISBOA S., JUNIOR M., CARVALHO B., SOUZA V., ROCHA C., ARAUJO F., 2019. Integrated Seismic-Log-Core-Test Fracture Characterization, Barra Velha Formation, Pre-salt of Santos Basin. Adapted from extended abstract prepared in conjunction with poster presentation given at 2019 AAPG Annual Convention and Exhibition, San Antonio, Texas, May 19-22.
- CORREIA ULISSES M.C., MELANI LEANDRO H., OLIVEIRA FELIPE M., LIMA LUANA G., KURODA MICHELLE C., CAMPANE ALEXANDRE VIDAL, 2019. The Impact of Faults, Fractures, And Karst in Carbonate Rocks: Examples from A Santos Basin Pre-Salt Reservoir. Tese, Universidade Estadual de Campinas.
- CORREIA, M. G., MASCHIO, C., SCHIOZER, D.J., 2017. Development of complex layered and fractured reservoir models for reservoir simulation. *Journal of the Brazilian Society of Mechanical Sciences and Engineering*, 39(1), 219-233, <https://dx.doi.org/10.1007/s40430-016-0606-7>.

- DAVISON, I., ANDERSON, L., NUTTALL, P., 2012. Salt Deposition, Loading and Gravity Drainage in the Campos and Santos Salt Basins. Geological Society Special Publication 363, 159–174. <https://doi.org/10.1144/SP363.8>
- DENG, X.L.; LI, J.H.; LIU, L.; REN, K.X., 2015. Advances in the Study of Fractured Reservoir Characterization and Modelling. *Geol. J. China Univ.*, 21, 306–319.
- DE JESUS, CANDIDA MENEZES, MARTINS COMPAN, ANDRE LUIZ, AND RODRIGO SURMAS, 2016. "Permeability Estimation Using Ultrasonic Borehole Image Logs in Dual-Porosity Carbonate Reservoirs." *Petrophysics* 57 (2016): 620–637.
- DE OLIVEIRA, R., & DOS SANTOS, A., 2017. Bacia de Santos, Agência Nacional do Petróleo, Gás Natural e Biocombustíveis, Brasil 14ª Rodada de Licitações da ANP.
- DERSHOWITZ, W. S., HERDA, H. H., 1992. Interpretation of fracture spacing and intensity. *Proceedings of the 33rd U.S. Symposium on Rock Mechanics*, eds Tillerson, J.R. and W.R. Wawersik, Rotterdam, Balkema. Pp. 757-766.
- DERHOWITZ, W., LA POINTE, P., DOE, T., 2007, *Advances in Discrete Fracture Network Modeling*, Golder Associates Inc.
- DUARTE, SANDRA BUZINI, DE JESUS, CANDIDA MENEZES, DA SILVA, VIVIANE FARROCO, AROUCA SOBREIRA, MATHEUS CAFARO, CRISTOFARO, RAPHAEL AGOSTIN LEITE, DE LIMA, LARISSA, DE MELLO E SILVA, FERNANDO GOMES, MARQUES DE SA, CARLOS HENRIQUE, DE OLIVEIRA BERTO, FLAVIO MARCOS, BACKHEUSER, YEDA, LOUREIRO, SEBASTIAO DE ANDRADE, DE ALMEIDA WALDMANN, ALEX T., AND LENITA DE SOUZA FIORITI. 2018. "Artificial Intelligence Use to Predict Severe Fluid Losses in Pre-Salt Carbonates." Paper presented at the SPWLA 59th Annual Logging Symposium, London, UK.
- GOMES, P. O., KILSDONK, B., MINKEN, J., GROW, T., BARRAGAN, R., 2008. The Outer High of The Santos Basin, Southern São Paulo Plateau, Brazil: Pre-

Salt Exploration Outbreak, Paleogeographic Setting, and Evolution of The Syn-Rift Structures. AAPG International Conference and Exhibition, Cape Town, South Africa 10193, 26–29.

HALLER, D. & PORTURAS, F. 1998. How to Characterize Fractures in Reservoirs Using Borehole and Core Images: Case Studies In: HARVEY, P. K. & LOVELL, M. A. (eds) Core-Log Integration, Geological Society, London, Special Publications, 136, 249-259.

HUAPENG NIU, SHICHEN LIU, JIN LAI, GUIWEN WANG, BINGCHANG LIU, YUQIANG XIE, WEIBIAO XIE, 2019. In-Situ Stress Determination and Fracture Characterization Using Image Logs: The Paleogene Dongying Formation in Nanpu Sag, Bohai Bay Basin, China, Energy Science & Engineering published by the Society of Chemical Industry and John Wiley & Sons Ltd; 8:476–489.

JAFARI, A.; KADKHODAIE-ILKHCHI, A.; SHARGHI, Y.; GHANAVATI, K., 2012. Fracture Density Estimation from Petrophysical Log Data Using the Adaptive Neuro-Fuzzy Inference System. J. Geophys. Eng. 2012, 9, 105–114.

KINGDON, A., FELLGETT, M.W., WILLIAMS, J.D.O., 2016. Use of Borehole Imaging to Improve Understanding of The In-Situ Stress Orientation of Central and Northern England And Its Implications for Unconventional Hydrocarbon Resources. Marine and Petroleum Geology, 73, 1-20.

LACOPINI, D., ALVARENGA, R., KUCHLE, J., GOLDBERG, K., and KNELLER, B., 2017. “Seismic Characterization of The Pre-Salt Rifted Section of The Lagoa Feia Group, Campos Basin, Offshore Brazil”. AAPG Annual Convention and Exhibition, Houston, Texas.

LAI, J., WANG, G., WANG, S., CAO, J., LI, M., PANG, X., HAN, C., FAN, X., YANG, L., HE, Z., QIN, Z., 2018. A Review on The Applications of Image Logs in Structural Analysis and Sedimentary Characterization. Marine and Petroleum Geology, 95,139-166.

- LEPLEY, S., PICCOLI, L., CHITALE, V., KELLEY, I., and QUEST, M., 2017. “The Importance of Understanding Diagenesis for The Development of Pre-Salt Lacustrine Carbonates”. AAPG Annual Convention and Exhibition, Houston, Texas.
- LIGTENBERG, J. H., 2005, Detection of fluid migration pathways in seismic data: implications for fault seal analysis, dGB Earth Sciences, Boulevard 1945 nr. 24, 7511 AE, Enschede, The Netherlands.
- MELLO, M. R., MACEDO, J. M., REQUEJO, R. and SCHIEFELBEIN, C., 2002, The Great Campos: A Frontier for New Giant Hydrocarbon Accumulations in the Brazilian Sedimentary Basins (Abstract), AAPG Bull, v. 85, no. 13, (Supplement
- MELDAHL, P., HEGGLAND, R., BRIL, B., AND PAUL G., 2001, Identifying Targets Like Faults and Chimneys Using Multi-Attributes and Neural Networks, Earth Sciences, Enschede, The Netherlands.
- MILANI, E. J., BRANDÃO, J. A. S. L., ZALÁN, P. V., & GAMBOA, L. A. P., 2000 Petróleo Na Margem Continental Brasileira: Geologia, Exploração, Resultados E Perspectivas. Brazilian Journal of Geophysics, vol. 18(3).
- MOREIRA, J. L. P., MADEIRA, C. V., GIL, J. A., MACHADO, M. A. P., 2007. Bacia de Santos. Boletim de Geociências. Petrobras, Rio de Janeiro, v. 15, n. 2, p. 531-549, maio/nov.
- MORLEY, C. K., NELSON, R. A., PATTON, T. L. E MUNN, S. G., 1990. Transfer Zones in The East African Rift System and Their Relevance to Hydrocarbon Exploration in Rifts: AAPG Bulletin, 74:1234–1253.
- NASSERI, A., MOHAMMADZADEH, M., RAEISI, H., 2015. Fracture Enhancement Based on Artificial Ants and Fuzzy C-Means Clustering (FCMC) in Dezful Embayment of Iran. J. Geophys. Eng. 2015, 12, 227–241.
- ODA, M., 1985. Permeability Tensor for Discontinuous Rock Masses. Geotechnique 35, 483–495, <https://dx.doi.org/10.1680/geot.1985.35.4.483>.

- OJEDA, H.A., 1982. Structural Framework, Stratigraphy and Evolution of Brazilian Marginal Basins. *American Association of Petroleum Geologists Bulletin* 66, 732-749.
- OLIVEIRA, T., CRUZ, N., CRUZ, J., CUNHA, R., MATOS, M., 2019. Faults, Fractures and Karst Zones Characterization in a Pre-Salt Reservoir using Geometric Attributes 1–5.
- PEREIRA, M.J., MACEDO, J.M., 1990. A Bacia de Santos: Perspectivas de Uma Nova Provincia Petrolífera Na Plataforma Continental Sudeste Brasileira. *Bol. Geociências Petrobras* 4, 3–11.
- PEREIRA, M.J., FEIJÓ, F.J., 1994. Bacia de Santos. Estratigrafia das Bacias Sedimentares do Brasil. *Bol. Geociências Petrobras* 8, 219–234.
- RIBEIRO, S., and PEREIRA, E., 2017. Tectono-Stratigraphic Evolution of Lapa Field Pre-Salt Section, Santos Basin (Brazilian Continental Margin). *Journal of Sedimentary Environments*, Published by Universidade do Estado do Rio de Janeiro.
- RICCOMINI, C., SANT, L.G., TASSINARI, C.C.G., 2012. Pré-Sal: Geologia e Exploração. *Revista USP* (95), 33-42.
- ROBERTS, A., 2001, Curvature attributes and their application to 3D interpreted horizons. *First Break*, 19, 85-99.
- SCHLUMBERGER, 2009B. Petrel 2009. Seismic to Simulation Software Manual: Seismic Visualization and Interpretation Course, Houston.
- SILVA, C., MARCOLINO, C., LIMA, F., SCHLUMBERGER, PETROBRAS, 2005. Automatic Fault Extraction Using Ant Tracking Algorithm in the Marlim South Field, Campos Basin. SEG/Houston 2005 Annual Meeting.
- VALENTINI, L., PERUGINI, D., POLI, G., 2007. The “small-world” topology of rock fracture networks. *Physica A: Statistical Mechanics and its Applications*, 377(1), 323-328, <https://doi.org/10.1016/j.physa.2006.11.025>.

VELTMAN, W., VELEZ, E., LUJAN, V., 2012. A Fresh Look for Natural Fracture Characterization Using Advance Borehole Acoustics Techniques. Adapted from extended abstract prepared in conjunction with oral presentation at AAPG Annual Convention and Exhibition, Long Beach, California, AAPG©2012.

ZALÁN, P. V., 2004. Evolução Fanerozóica Das Bacias Sedimentares Brasileiras. Petrobras, E&P, E&P-Exp, GPE, NNE, Rio de Janeiro, RJ.

ZALÁN, P. V., OLIVEIRA, J. A. B., 2005. Origem E Evolução Estrutural Do Sistema De Riftes Cenozoicos Do Sudeste Do Brasil. Boletim de Geociências da Petrobras, Rio de Janeiro, v. 13, n. 2, p. 269-300, maio/nov.

CONCLUSIONS

The pre-salt play is primarily composed of lacustrine carbonates with high permeability controlled by fracture intensities and carbonate dissolution, with this was possible to create a discrete fracture network (DFN) model that captures the intensity, orientation, and spatial distribution of fractures, allowing estimates of permeability and secondary porosity. The constructed model can be used in future reservoir simulation studies to better understand and improve reservoir productivity.

The use of seismic attributes and borehole image logs allowed for the main inputs of the DFN to be identified. These inputs include the interpretation of natural fractures, the definition of the in-situ stress state in the pre-salt play, and the interpretation of the pre-salt play horizons, which comprise the top and base of the model (Barra Velha and Camboriu formations), and regional faults. Based on the findings, we conclude that, consistent with borehole breakouts and drilling-induced fractures, the maximum horizontal stress (SHmax) has an azimuth of NE-SW, indicating that the study area is influenced by a normal fault pattern and extensional stress configuration when compared to the orientation and regime of large structures of seismic scale in the reservoir. Moreover, we identified four sets of natural fractures, of which F1 and F2 sets strike parallel to SHmax NE-SW and had the maximum permeability responses in the same direction, suggesting good connection for the fractures belonging to these two structural systems.

It is worth noting that the results of permeability and porosity developed from the DFN require calibration with well tests, and the outputs from this work can be utilized to build geomechanical reservoir models that help comprehend matrix-fracture relationships for wellbore stability.

APPENDIX 1 - INTERPRETATION OF NATURAL FRACTURES, BREAKOUTS AND DRILLING INDUCED FRACTURES

The interpretation of fractures in this thesis was based on Borehole images logs by acoustic tools acquired from Circumferential Acoustic Scanning UBI (Ultrasonic Borehole Imager). The data was loaded, calibrated according to magnetic declination and accelerometer to provide the true orientation and the structures were interpreted.

Natural fractures were primarily observed as structures with a consistent orientation and are often symmetrically distributed along the entire wellbore section; breakouts are represented by continuous dark zones where the borehole wall was collapsed; and drilling-induced fractures have a sub-parallel or slightly inclined orientation to the borehole axis, do not fully cross the wellbore, and have an asymmetrical distribution.

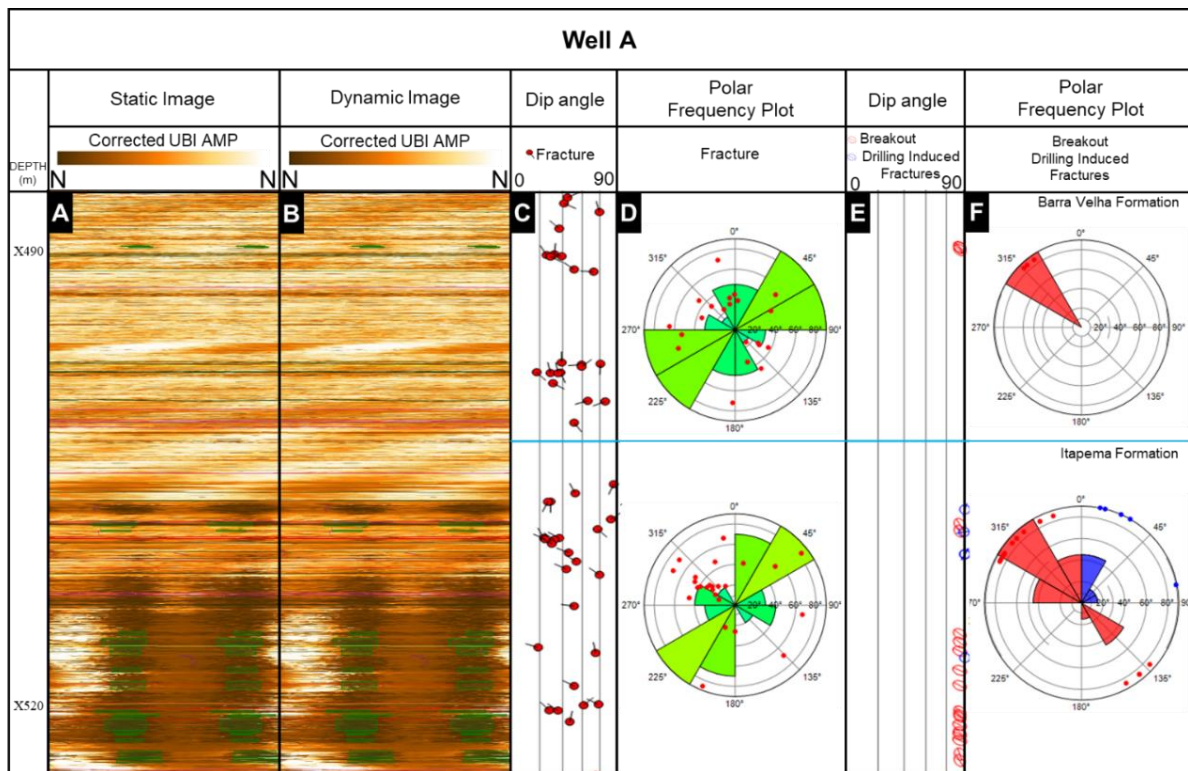


Figure 35. Interpreted natural fractures, breakouts and drilling induced fractures at well A. A) Static image log. B) Dynamic Image log. C) Dip angle of natural fractures in tadpole. D) Rose diagram of the natural fractures showing strike azimuth. E) Dip angle of breakouts and drilling induced fractures in tadpole. F) Rose diagram of breakouts and drilling induced fractures showing strike.

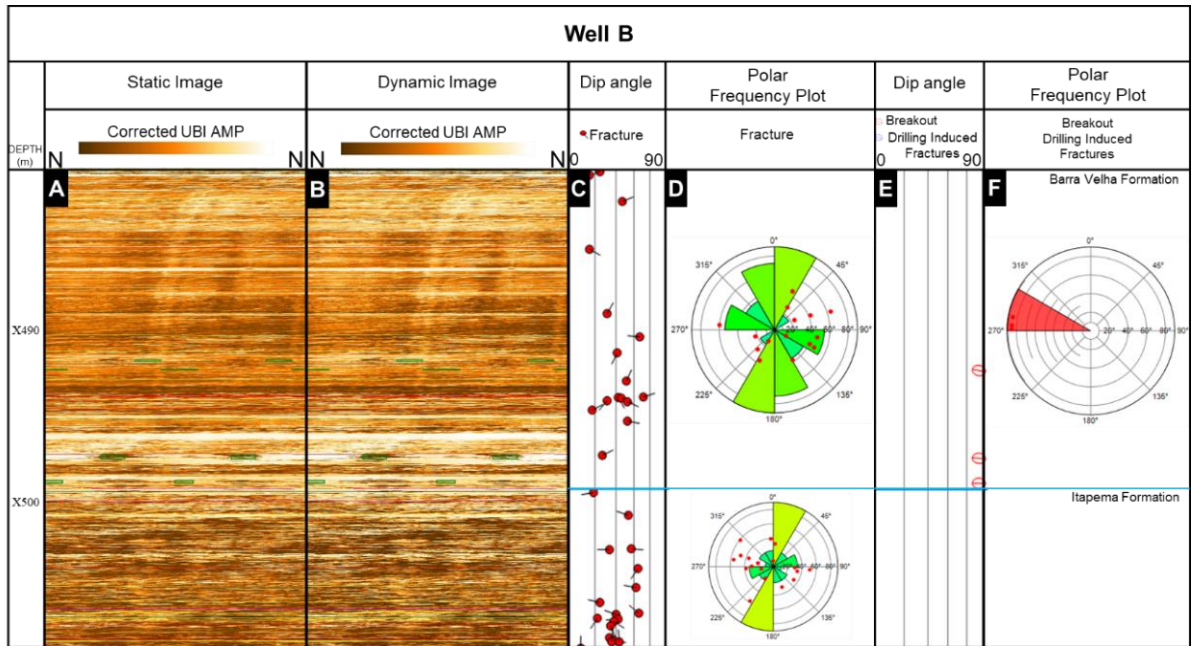


Figure 36. Interpreted natural fractures, breakouts and drilling induced fractures at well B. A) Static image log. B) Dynamic Image log. C) Dip angle of natural fractures in tadpole. D) Rose diagram of the natural fractures showing strike azimuth. E) Dip angle of breakouts and drilling induced fractures in tadpole. F) Rose diagram of breakouts and drilling induced fractures showing strike.

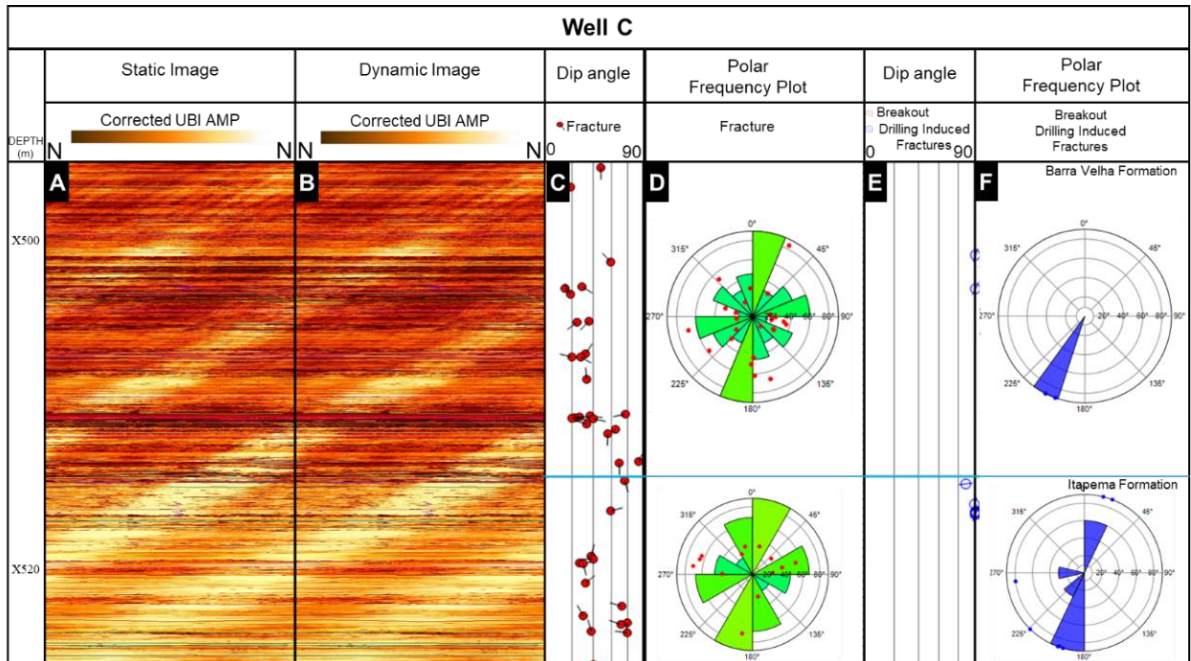


Figure 37. Interpreted natural fractures, breakouts and drilling induced fractures at well C. A) Static image log. B) Dynamic Image log. C) Dip angle of natural fractures in tadpole. D) Rose diagram of the natural fractures showing strike azimuth. E) Dip angle of breakouts and drilling induced fractures in tadpole. F) Rose diagram of breakouts and drilling induced fractures showing strike.

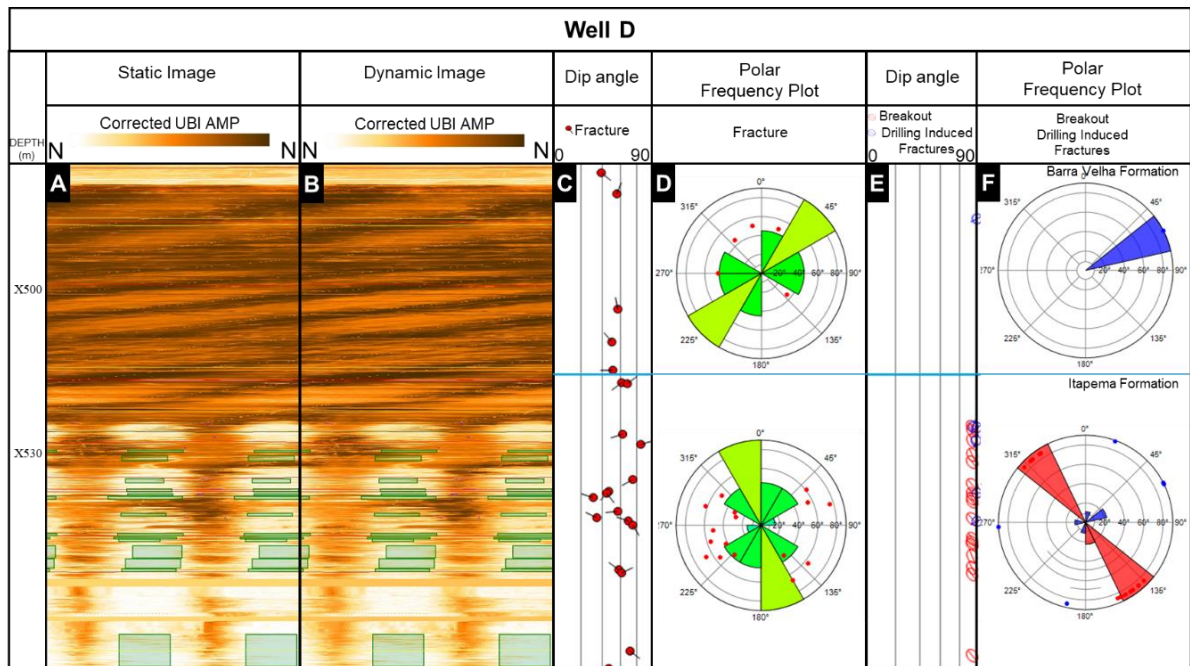


Figure 38. Interpreted natural fractures, breakouts and drilling induced fractures at well D. A) Static image log. B) Dynamic Image log. C) Dip angle of natural fractures in tadpole. D) Rose diagram of the natural fractures showing strike azimuth. E) Dip angle of breakouts and drilling induced fractures in tadpole. F) Rose diagram of breakouts and drilling induced fractures showing strike.

APPENDIX 2 – ANT TRACKING WORKFLOW

Schlumberger created the Ant Tracking algorithm. This algorithm mimics how ant colonies in nature use pheromones to mark their paths in order to optimize their search for food. Similarly, virtual ants are used as 'seeds' on a seismic discontinuity volume to detect fault zones. The ants use virtual pheromones to collect information about the fault zones in the volume. Because it enhances horizon discontinuities, the result is an attribute volume with very sharp and detailed fault zones. (Silva and colleagues, 2005).

The following ant-tracking workflow was used in this thesis: the first process is preconditioning the seismic volume, which involves noise removal to improve the signal-to-noise ratio and obtain better reflector continuity, allowing the ants to isolate discontinuous zones more easily; next, an attribute such as variance or chaos is required to highlight discontinuities, and this is the input to finally generate the ant tracking volume, in order to obtain the fault patches

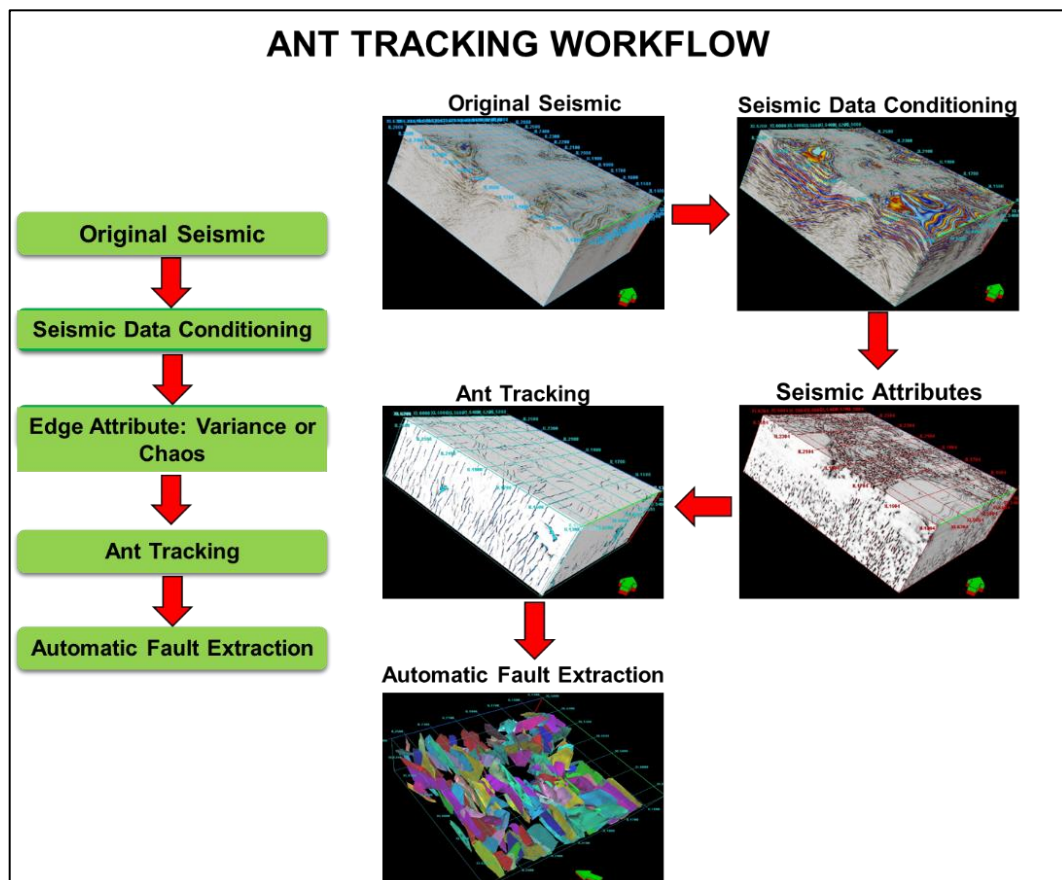


Figure 39. Ant-Tracking Workflow.

APPENDIX 3 – SEISMIC DATA CONDITIONING

In this thesis, the seismic volume was preconditioned by applying filters to eliminate seismic anomalies such as acquisition footprints or multiples; the process was based on the evaluation of 3D seismic data mostly through amplitude maps and amplitude spectra.

At first, a semi-automated geostatistical filter (Destriping Filter) was used, which used factorial kriging to filter out noise using local noise and signal characteristics. Following that, the structure-oriented filter (SOF) is used to remove random noise from the data by aligning the seismic reflector using the dip-steering technique, thus increasing the structural and stratigraphic properties (Chopra and Marfurt, 2008). Finally, the Dip Steered Median Filter (DSMF) is used, which changes the diffuse terminations of the reflectors closer to the fault zones with a pre-computed geometry feature, which recognizes the dissimilar seismic traces and improves the reflectors' edge (Jaglan and Qayyum, 2015)

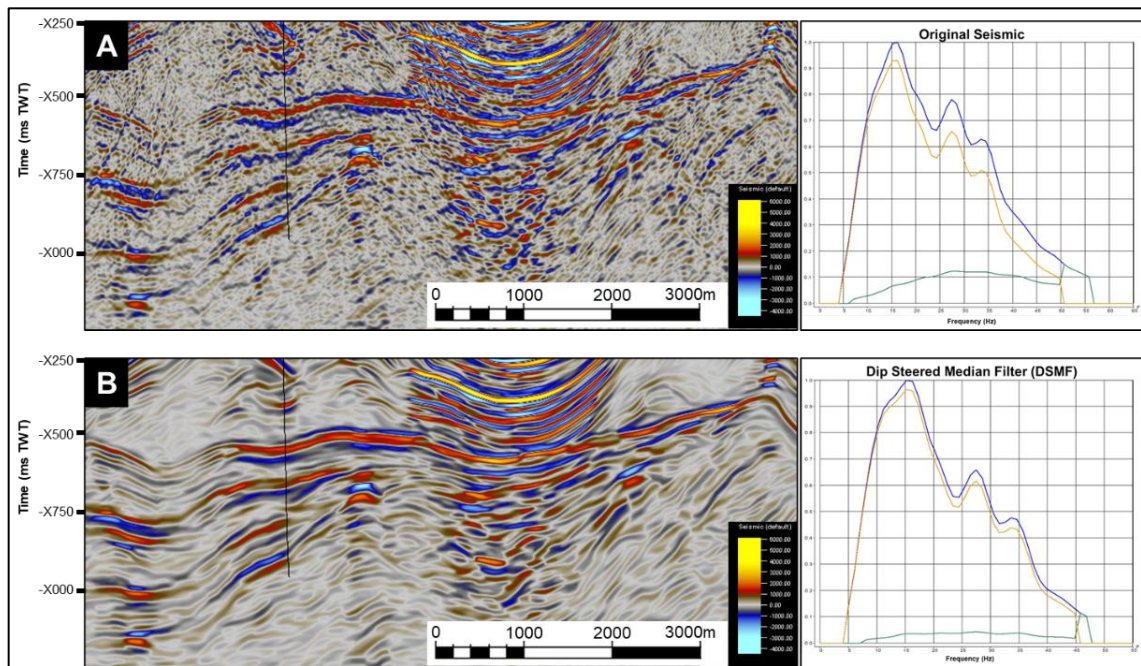


Figure 40. Comparison amplitude spectra. A) Original seismic. B) Dip-Steered Median Filter (DSMF).

REFERENCES

- CHANG, H.K., KOWSMANN, R.O., FIGUEIREDO, A.M.F.& BENDER, A.A., 1992. Tectonics and Stratigraphy of The East Brazil Rift System (EBRIS): an overview. *Tectonophysics* 213, 97-138.
- CORREA R., PEREIRA C., CRUZ F., LISBOA S., JUNIOR M., CARVALHO B., SOUZA V., ROCHA C., ARAUJO F., 2019. Integrated Seismic-Log-Core-Test Fracture Characterization, Barra Velha Formation, Pre-salt of Santos Basin. Adapted from extended abstract prepared in conjunction with poster presentation given at 2019 AAPG Annual Convention and Exhibition, San Antonio, Texas, May 19-22.
- GHOSH, K., MITRA, S., 2009. Structural Controls of Fracture Orientations, Intensity, And Connectivity, Teton Anticline, Sawtooth Range, Montana. *AAPG bulletin*, 93(8), 995-1014,
- GOMES, P. O., KILSDONK, B., MINKEN, J., GROW, T., BARRAGAN, R., 2008. The Outer High of The Santos Basin, Southern São Paulo Plateau, Brazil: Pre-Salt Exploration Outbreak, Paleogeographic Setting, and Evolution of The Syn-Rift Structures. *AAPG International Conference and Exhibition, Cape Town, South Africa* 10193, 26–29.
- GONG, J., ROSSEN, W.R., 2018. Characteristic Fracture Spacing in Primary and Secondary Recovery for Naturally Fractured Reservoirs. Department of Geoscience & Engineering, Delft University of Technology, Delft 2628 CN, The Netherlands.
- GUTIÉRREZ, Z., 2016. Efecto del Espaciamiento y Longitud de Fracturas Sobre la Permeabilidad de un Yacimiento Naturalmente Fracturado: Caso Piedemonte Llanero Colombiano. Universidad Nacional de Colombia, Facultad de Minas, Departamento de Procesos y Energía. Medellín, Colombia.
- JAGLAN, H., QAYYUM, F., 2015. Unconventional Seismic Attributes for Fracture Characterization. *First Break* 33, 101–109.

- LIGTENBERG, J. H., 2005, Detection of fluid migration pathways in seismic data: implications for fault seal analysis, dGB Earth Sciences, Boulevard 1945 nr. 24, 7511 AE, Enschede, The Netherlands.
- MELDAHL, P., HEGGLAND, R., BRIL, B., AND PAUL G., 2001, Identifying Targets Like Faults and Chimneys Using Multi-Attributes and Neural Networks, Earth Sciences, Enschede, The Netherlands.
- OJEDA, H.A., 1982. Structural Framework, Stratigraphy and Evolution of Brazilian Marginal Basins. American Association of Petroleum Geologists Bulletin 66, 732-749.
- SILVA, C., MARCOLINO, C., LIMA, F., SCHLUMBERGER, PETROBRAS, 2005. Automatic Fault Extraction Using Ant Tracking Algorithm in the Marlim South Field, Campos Basin. SEG/Houston 2005 Annual Meeting.